Ion transport in microbial fuel cells: Key roles, theory and critical review

Manon Oliot *, Sylvain Galier, Hélène Roux de Balmann, Alain Bergel

Laboratoire de Génie Chimique, Université de Toulouse, CNRS, INP, UPS, France

HIGHLIGHTS

- MFC behaviour is predicted from the analysis of the electrolyte content.
- The theoretical concept of transport number is detailed.
- A comprehensive classification is provided of separators reported in MFCs.
- The experimental effects of the various separators are compared with theory.
- Future research directions are recommended.

ABSTRACT

Microbial fuel cells (MFCs) offer the possibility to convert the chemical energy contained in low-cost organic matter directly into electrical energy. Nevertheless, in the current state of the art, microbial electrocatalysis imposes the use of electrolytes of low ionic conductivity, at around neutral pH and with complex chemical compositions, which are far from being ideal electrolytes for an electrochemical process. In this context, ion transport through the electrolyte is a key step, which strongly conditions the electrode kinetics and the global cell performance.

The fundamentals of ion transport in electrolytes are recalled and discussed in the light of MFC constraints. The concept of transport number is emphasized in order to provide an easy-to-use theoretical framework for analysing the pivotal roles of ion transport through the electrolyte. Numerical illustrations show how the concept of transport number can be used to predict MFC behaviour on the basis of the electrolyte composition. The tricky problem of pH balance is discussed, the interest of separator-less MFCs is emphasized, and the concept of "microbial separator" is proposed as a worthwhile future research direction.

The role of separators in driving ion transport is then reviewed following a comprehensive classification, from the most compact, non-porous membranes to the most porous separators. For each group, basic are first recall to guide the critical analysis of the experimental data. This analysis brings to light a few research directions that may be reoriented and some critical issues that need in-depth investigation in the future. The suitability of cation-/anion-exchange membranes is discussed in comparison to that of porous separators. Finally, the large discrepancy observed on data obtained for the same separator type suggests that, in the future, specific analytical set-ups should be developed.

Contents

1. Introduction

For around 15 years, it has been known that microbial biofilms can act as electrocatalysts and be very efficient in this role [1–5]. Microbial electrocatalysis makes possible electrochemical reactions that "abiotic electrochemists" would never have dared to imagine before, such as the oxidation of acetate, organic fatty acids, and sugars [6,7] or the reduction of carbon dioxide to acetate, ethanol and fuels [8,9]. Numerous reviews have presented the wonderful perspectives opened up by microbial electrochemical technology [10] in a wide variety of application domains [11–13], and particularly for the production of renewable energy from non-fossil sources. Microbial fuel cells (MFCs) can convert the chemical energy contained in low-cost organic matter directly into electrical energy [14,15], microbial electrolysis cells can produce hydrogen from the same renewable, low-cost compounds [16,17], and microbial electrosynthesis cells [8,9,18] can use carbon dioxide to store electrical energy in chemical form.

Microbial fuel cells (MFCs) are considered as the archetype of microbial electrochemical technologies [19] for several reasons. Firstly, the beauty of the concept of transforming the chemical energy contained in organic matter directly to electricity is doubtless a reason for its success. Secondly, MFCs were the pioneering systems at the origin of microbial electrochemical technologies [2–4,20]. Finally, MFCs can be cheap devices. The microbial anode, often graphite, does not involve expensive materials and the electrocatalytic biofilm forms spontaneously on its surface from the microorganisms contained in the electrolyte, without requiring any sophisticated chemical procedure. The cathode can be abiotic or biotic [19,21], most often achieving oxygen reduction. As an MFC produces its own current, monitoring does not require expensive electrochemical equipment. Measuring the current and the cell voltage may be sufficient for a first, simple approach. Although an MFC cannot be assimilated with an electroanalytical system [22], it has had the advantage of opening up the exciting field of electroactive biofilms to a large variety of research groups. The number of papers referring to MFCs has increased continuously year on year, reaching more than 1000 articles published last year.

Any electrochemical process is based on a continuous chain composed of three successive steps: (i) electron transfer from the cathode to dissolved species, (ii) ion transport through the electrolyte and (iii) electron transfer from dissolved species to the anode. For each electron that is released from the cathode and collected at the anode a positive ionic charge must move to the cathode or a negative ionic charge must move to the anode (Fig. 1). The slowest step(s) in this chain controls the system performance. If ion transport in the electrolyte is not fast enough, it can severely limit the electron transfer rate at the electrodes. The rate of electrochemical reactions depends straightforwardly on the capacity of the electrolyte to ensure efficient ion transport. The risk of ion

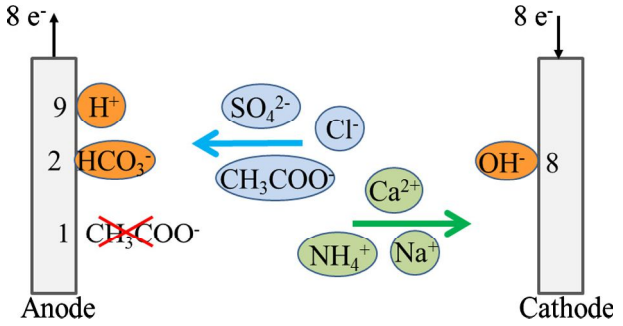

Fig. 1. Scheme of ion transport pattern in an electrolyte with a chemical composition roughly representative of wastewater with 5 mM sodium acetate added, pH 7.0: Na^+ 6 mM, Ca^{2+} 3.2 mM, NH_4^+ 3.6 mM, H^+ 10^{-4} mM, CH_3COO^- 5 mM, Cl^- 4 mM, SO_4^{2-} 3.5 mM, OH^- 10^{-4} mM. Transport numbers were: Na^+ 14.9%, Ca^{2+} 18.9% (z = 2), NH_4^+ 13.1%, H^+ 0%, CH_3COO^- 10.1%, Cl^- 15.1%, SO_4^{2-} 27.8% (z = 2), OH^- 0%. For the scheme presented on the basis of 8 exchanged electrons, the transport numbers corresponded to molar flux around 1 ion for each species, except H^+ and OH^-. Ionic conductivity of the electrolyte was 0.20 S m^{-1}.

transport being rate-limiting increases with decreasing ionic conductivity of the electrolyte.

Introducing a biofilm into an electrochemical process considerably increases the level of complexity of each step by imposing new constraints related to microbial growth. The kinetics of electron transfer at microbial anodes and microbial cathodes have been the subject of very many studies, which have led to remarkable fundamental and technical advances [23,24]. In comparison, the new constraints that biofilm catalysis imposes on ion transport through the electrolyte have been less comprehensively evaluated so far.

Microorganisms generally grow in solutions at around neutral pH and do not tolerate high salinity. In consequence, most MERs use electrolytes at around neutral pH and low salinity, which means electrolytes with low ionic conductivity. The large majority of MERs have so far been implemented in synthetic culture media with conductivity of the order of 1 S m^{-1} [25,26] but the conductivity can fall lower than 0.06 S m^{-1} [27,28] when wastewater is used as the electrolyte. In comparison, the electrolytes used in conventional electrochemical reactors (abiotic processes) have ionic conductivities of several tens of S m^{-1}. For example, 10–33% KOH, which is commonly used for water electrolysis, has conductivity of up to 60 S m^{-1}. The low ionic conductivity of the electrolyte used in microbial electrochemical reactors (MERs) has often been identified as a major drawback.

Ion transport through the electrolyte costs energy, which is lost as heat. The power consumed by the ion motion through the electrolyte is inversely proportional to the conductivity of the electrolyte (see Eq. (15)). A decrease of conductivity of one, two or up to three orders of magnitude, as is the case for MERs in comparison with conventional abiotic electrochemical reactors, leads directly to an increase of the same proportion in power loss. For example, when 33% KOH is used as the electrolyte in an abiotic electrochemical reactor, a current density of 100 A m^{-2} between an anode and a cathode that are 1 cm apart creates an ohmic drop of less than 17 mV, i.e. a power loss of 1.7 W m^{-2}. In similar conditions, a MER using an electrolyte of 1 S m^{-1}conductivity would induce an ohmic drop of 1000 mV, i.e. a power loss of 100 W m^{-2}. This elementary calculation shows how essential the issue of ion transport through the electrolyte is, and how severely it can impact the large-scale development of microbial electrochemical technologies.

A reduction of the power loss due to ion transport can be achieved by reducing the distance to be travelled by the ions, i.e. the distance between anode and cathode (see Eq. (15)). Nevertheless, in most MERs, the chemical composition of the anode electrolyte must be different from the composition of the cathode electrolyte. These two opposite objectives, decreasing the inter-electrode distance while keeping chemical gradients between anode and cathode, are commonly pursued by using a separator between anode and cathode.

A large diversity of separators of various natures has been screened in the context of MERs, and reviewed in several recent articles. Reviews by Dhar and Lee [29] or Daud et al. [30] have thus analysed the major technical barriers related to membranes in MERs. Other review articles have focused on MFCs: Li et al. [31] have listed the different separator configurations while Leong et al. [32] have detailed the effects of separators on MFC performance. Recently, a review has focused specifically ceramic material, which has the great advantage of being usable as the structural material, the electrode material and also the ion exchange medium [33]. Integration of membranes into MFC designs, such as cation-exchange membranes, anion-exchange membranes, or osmosis membranes can bestow an additional function on an MFC or even fully transform its essential objective. In this context, MFCs designed for water reclamation, saline water desalination and wastewater treatment have been reviewed by Yuan and He [34], Sevda et al. [35] and Xu et al. [36], respectively. A different kind of approach has been proposed by Varcoe et al. [37], who considered only anion exchange membranes used as the separator and reviewed the applications of this separator in all kinds of fuel cells, including both chemical and microbial fuel cells.

Reviews of separators in MERs, and specifically MFCs, have mainly focused on the technical aspects of separators and their experimental impact on the MER behaviour and performance. Some attempts at theoretical modelling have started to be proposed. Ion transport through an ion-exchange membrane has been modelled numerically [38] and a theoretical approach has also shown the impact of buffer transport through the electrolyte on the cathode overpotential [39]. Harnisch and Schröder have proposed a detailed description of the intricate effects of ion transport on the other phenomena that control the behaviour of an MER, particularly emphasizing the problem of pH splitting between the anode and cathode zones [40]. Recently, Popat and Torres have shaped the general framework of all the transport phenomena that can be rate-limiting steps in MERs, including electron transport and mass transports occurring inside the electroactive biofilms [41]. These studies have confirmed the pivotal role of ion transport through the electrolyte in MERs. Nevertheless, the theory of ion transport in electrolytes has rarely been used to develop a unified theory to analyse the huge amount of experimental data reported in the literature.

Curiously, to the best of our knowledge, transport numbers have never been used so far in the context of MERs, although they are very useful theoretical tools, widely used to investigate ion transport in electrochemical and membrane processes. The transport number concept offers a simple theoretical approach to ion transport in electrolytes and gives an easy-to-handle theoretical basis for analysing experimental data and, very interestingly, for predicting some aspects of the behaviour of an electrochemical reactor based on the analysis of the electrolyte composition.

The objectives of the present review are, firstly, to provide a simple theoretical tool to tackle the thorny problem of ion transport in MFCs and, secondly, to review the experimental data reported in the literature from the standpoint of this theoretical basis. The theoretical explanation is based on MFCs but the approach and the main conclusions should also be useful for other kinds of MERs. Fundamentals of MFCs are briefly recalled by emphasizing how the specific electrolytes required for microbial growth can impact the anode and cathode electrochemical behaviours and how ion transport through the electrolyte can enhance or mitigate these phenomena.

The concept of transport numbers is presented and used as a theoretical breadcrumbs trail to analyse ion transport in MFC in the absence or presence of a separator. In each case, theory is firstly used to anticipate how ion transport through the electrolyte may impact the MFC behaviour. This theoretical basis is then used for a critical review of the experimental data reported in the literature. Confronting experimental data with theoretical expectations points out predictable data that fit the theory and others, which seem rather surprising and need further investigation. As a result of this cross analysis, advice for enhancing or reorienting some current approaches is given and key issues for progressing towards mastery of ion transport in MFCs are proposed. The objective is to stimulate thinking and discussion in order to boost the advance of electrochemical technology towards practical applications.

2. Back to basics

2.1. Electrolytes of MERs vs. abiotic electrochemical reactors

The solutions used in MFCs are very different from the electrolytes used in conventional abiotic electrochemical processes. Abiotic electrochemical reactors generally implement solutions with very simple chemical compositions in order to avoid fouling and inhibition of the electrocatalytic surfaces. Metallic electrocatalysts are known to be very sensitive to any source of pollution and most of them require clean reactants. In contrast, microbial electrodes are most often developed in very complex media, even in "dirty" solutions such as marine sediments or wastewaters, the composition of which is sometimes not fully known. Even when bioelectrodes are formed from pure cultures, complex media must be used, which must contain all the micro-nutriments and trace elements required for microbial growth. Consequently, MER electrolytes generally contain various chemical compounds, and Ca^{2+}, Mg^{2+} and other cations.

As mentioned in the introduction of this article, electroactive biofilms are generally sensitive to high salinity and are consequently developed in solutions of low conductivity. A few recent articles have described halotolerant electroactive biofilms able to work in solutions with ionic conductivity higher than 10 S m^{-1} [25,42]. Benthic MFCs operate in seawater [43,44] but the energy they produce remains modest because of the low availability of organic matter in sediment. Nevertheless, the large majority of MFC electrolytes have conductivities in the range of 0.5–2 S m^{-1} [25,26]. When wastewater is used as the electrolyte, ionic conductivity is as low as 0.15 S m^{-1} [45,46] and even lower than 0.06 S m^{-1} [27,28]. In comparison, abiotic electrochemical processes commonly used electrolytes with conductivities two to three orders of magnitude higher.

Finally, using a microbial biofilm as the electrocatalyst most often makes it indispensable to work at pH values around neutrality. Some electroactive biofilms can develop in slightly alkaline solutions [47–50] but, except for a few cases up to pH 11 [51], generally not above pH 10. Very few have been formed in acidic solutions below pH 5 [28,47]. In consequence most MFCs work at pH values around 7–8.

In summary, the need to develop and to maintain living biofilms in MFCs imposes three main constraints on the electrolytes:

- complex chemical composition, including cations,
- low conductivity,
- pH around neutrality,

which represent three new and awkward conditions in the context of electrochemistry.

2.2. Microbial anode

2.2.1. Electron transfer and limitation due to local acidification

On the anode of an MFC, the microbial biofilm oxidizes the organic substrate(s) by transferring the electrons produced to the anode material. Acetate has been widely used as an MFC substrate [6] and can be taken as a model:

$$CH_3COO^- + 4H_2O \rightarrow 2HCO_3^- + 9H^+ + 8e^- \quad (1)$$

The electrochemical reaction provokes acidification of the solution near the anode surface. The local pH decrease inside the biofilm creates adverse conditions for microbial development and severely affects the electrocatalytic activity of the biofilms. This is a major limitation of the anode performance because very few electroactive biofilms have been shown to be efficient at pH values under 5 [47].

The detrimental effect of local acidification inside the biofilms of bioanodes has already been pointed out and theorized [40,41,52]. Nevertheless, ion transport inside biofilms is outside the scope of this review. This is of great interest but it would deserve specific in depth investigations because ion transport inside the biofilm matrix may be complicated by the accumulation of different compounds coming from the solution or produced by the cells, including, for instance, weak acids, which may contribute to the pH balance. The present study addresses ion transport through the bulk electrolyte of MFCs. The anode and cathode are considered as the boundaries of the electrolyte. The electroactive biofilm that develops at the anode, and at the cathode if a biocathode is implemented, is assumed to be part of the electrode kinetics and is not assimilated as part of the electrolyte [53].

2.2.2. Deactivation by oxygen

A microbial anode requires an anaerobic environment. A microbial anode may involve strictly-anaerobic anode-respiring bacteria, which are killed by the presence of oxygen. On the other hand, some electroactive bacteria can tolerate oxygen. In this case, the presence of oxygen diverts them from electron transfer to the anode and electrons are preferentially released to oxygen [40]. They prefer oxygen, their natural electron acceptor, over the electrode material. In supplement, oxygen can also support the development of non-electroactive bacteria in the biofilm or on its external side [54]. The growth of aerobic bacteria thickens the biofilm, which may distend the extracellular electron transport network and hinder mass transfer of the fuel to the anode-respiring bacteria. Consequently, in an MFC, either by killing the cells or diverting them to electron transfer to the electrode or by favouring the development of non-electroactive cells, the flux of oxygen to the anode can severely affect the electrocatalytic performance.

2.3. The cathode

2.3.1. Electron transfer and limitation due to local alkalinization

Electrons collected at the anode flow through the external electrical circuit and are re-injected to dissolved species at the cathode. Oxygen is the most common oxidizer used at MFC cathodes. Many cathodes used in MFCs are abiotic and use an inorganic catalyst such as platinum, although it loses most its efficiency at the around neutral pH required in MFCs. Looking for oxygen-reduction catalysts that are efficient at neutral pH is a hot research topic [55], and many studies have aimed at finding less expensive and more efficient inorganic catalysts [56–58], including simply activated carbon [59] or more technologically-advanced materials such as graphene [60]. These abiotic cathodes are often implemented in the form of air-cathodes, with one side exposed to the electrolyte and the other side exposed to air [61]. Microbial oxygen-

reducing cathodes may be another solution of interest [21,62] and enzymatic cathodes have also been envisioned [19,63]. Two mechanisms of oxygen reduction are possible, depending on pH:

$$O_2 + 4e^- + 4H^+ \rightarrow 2H_2O \quad (2)$$

$$O_2 + 4e^- + 2H_2O \rightarrow 4OH^- \quad (3)$$

Eq. (2) has frequently been used in MFC studies, mainly in pioneering works, where it was probably chosen by similarity with proton exchange membrane fuel cells (PEMFCs). However, the pH of an MFC electrolyte is very different from that in a PEMFC as the development of the microbial biofilms imposes pH close to neutrality. Proton concentration is rarely higher than 10^{-6} M in an MFC, which is not sufficient to sustain mechanism (2). Except in the few rare cases that have implemented oxygen-reducing cathodes in acidic conditions [64], the reduction of oxygen in an MFC should be considered according to mechanism (3), i.e. as a reaction that produces OH^- ions.

Thermodynamically, the pH increase near the cathode surface is detrimental to the oxygen reduction reaction [65]. Alkalinization of the cathode zone has an additional disadvantage in MFCs. It is known that the pH increase leads to the precipitation of cations on the surface of oxygen-reducing cathodes in the form of hydroxides and scale [66,67]. Cations such as Ca^{2+} or Mg^{2+}, which are commonly present in the culture, are sources of surface fouling of MFC cathodes by alkaline precipitation. The phenomenon will be all the stronger when OH^- ion production is high, that is to say it will become stronger as the current increases. In particular, this phenomenon may limit the performance of benthic MFCs because of the high proportions of these cations in seawater [68,69].

From the experimental point of view, even if the current provided by MFCs remains rather low in the present state of the art, chemical fouling of the cathode has already been observed [70,71]. A recent study has evidenced sodium carbonate and calcium carbonate deposits on the air-side and the water-side of an MFC air-cathode, respectively, and showed their major role in decreasing the cathode performance [72].

2.3.2. Deactivation by organic matter

In the absence of a separator, the cathode is exposed to the organic matter contained in the electrolyte. However, even when a separator is used, the cathode may be exposed to organic matter, e.g. fuel, which flows through the separator, depending on its nature. The mechanisms of deactivation of the cathode may be different for abiotic and microbial cathodes.

For abiotic cathodes, the presence of organic compounds can be a source of conventional inhibition. Metallic catalysts of oxygen reduction, such as platinum, are known to be very sensitive to organic pollution [73]. The formation of mixed potentials due to simultaneous catalysis of oxygen reduction and the oxidation of organic compounds also results in a lowering of the cathode performance [74]. Biocathodes using pure enzymes as catalysts can be affected by the same kind of inhibition mechanism [75] as, similarly to metallic catalysts, enzymes are known to be very sensitive to inhibition.

Cathodes generally work in non-sterile conditions. If they are provided with organic compounds, a biofilm develops on the cathode surface, which can hinder mass transfers to or from the electrode [76,77]. When an air-cathode is used, the parasitic biofilm can develop either on the side exposed to the electrolyte or on the side exposed to air. In the first case, mass transfer of the OH^- ions (Reaction (3)) from the surface [70,78] is hindered by the biofilm; in the second case biofouling hinders the mass transfer of oxygen to the catalyst [78,79]. Nevertheless, in some cases, the biofilm has been observed to become virtuous by acquiring oxygen electrocatalytic ability [80].

For microbial cathodes, the presence of organic compounds can lead the oxygen-reducing electroactive bacteria to preferentially use the fuel, rather than the cathode, as the electron donor [81]. This phenomenon is similar to the deactivation of microbial anodes by the presence of oxygen. On the other hand, the presence of both oxygen (electron acceptor) and organic matter (possible electron donor) favours the development of non-electroactive bacteria, which can thicken the biofilm, disturb the electron transport mechanisms and slow down mass transfers.

2.4. Theoretical basis of ion transport in electrolytes and transport number

2.4.1. Importance of ion transport in the electrolyte bulk

The balance sheet of reactions (1) and (3) shows that positive charges are created at the anode, while the same quantity of negative charges is created at the cathode. To maintain electroneutrality, an equivalent amount of anions must be transported to the anode or cations to the cathode. The motion of ions through the electrolyte is the only way to carry electricity inside the MFC. If ion transport through the electrolyte is low, it can drastically limit the rate of electron transfer at the electrodes. Electron transfers at the electrodes cannot be faster than ion transport through the electrolyte.

In chemical hydrogen fuel cells, ion transfer is rather simple, because the protons produced at the anode by hydrogen oxidation migrate to the cathode where they are involved in oxygen reduction (Reaction (2)) [82]. The flux of protons produced at the anode is equal to the flux of protons transported through the electrolyte and to the flux of protons consumed at the cathode.

In MFCs the situation is far more complex due to the specificity of the electrolyte imposed by microbial growth requirements (Section 2.1). Around neutral pH, the contribution of protons and hydroxide ions to electricity carrying through the bulk is nil (see Section 3.4.1); the anode produces protons, the cathode produces hydroxide ions, but other ions ensure ion transport through the electrolyte (Fig. 1). As a result, a sharp pH split can occur between the anode zone, which acidifies (Section 2.2), and the cathode zone, which alkalinizes (Section 2.3). The possible pH buffering of these two zones depends on the way buffer species are transported through the bulk. Moreover, the fuel, most often acetate or other dissociated volatile fatty acids, can also be involved in ion transport through the bulk. The flux of fuel to the anode and the detrimental effect of the fuel flux to the cathode (Section 2.3.2) can thus be strongly impacted by their transport through the electrolyte. Similarly, the possible biofouling of the cathode by the precipitation of cations also depends on the way these cations are transported through the electrolyte.

In summary, because of the low ionic conductivity of MFC electrolytes, ion transport may be a rate-limiting step of the electrochemical chain. Moreover, because of the neutral pH and the chemical complexity of the MFC electrolytes, ion transport through the bulk is at the crossroad of multiple fluxes, which directly impact the operating conditions of the electrodes. Ion transport through the electrolyte is clearly an essential step, which must be optimized if the objective is to design efficient MFCs.

2.4.2. Ion transport, general theory

The motion of the ionic species ensures current transport through the electrolyte(s), each ionic species carrying a current density (J_i) proportional to its charge:

$$J_i = z_i F \phi_i \quad (4)$$

where the subscript i refers to the species i, J_i is the current density (A m^{-2}), z_i is the charge (e.g. +1 for Na^+, −1 for Cl^-), F is Faraday's constant (96,485 C mol^{-1}), ϕ_i is the molar flux (mol m^{-2} s^{-1}).

The molar flux of species i (ϕ_i) is described through the Nernst-Planck equation:

$$\phi_i(x) = -D_i \frac{\partial a_i(x)}{\partial x} - \frac{z_i F}{RT} D_i C_i \frac{\partial \varphi(x)}{\partial x} + C_i \upsilon(x) \quad (5)$$

where D_i is the diffusion coefficient ($m^2\ s^{-1}$), a_i is the activity (no unit), x is the distance along the X-axis, z_i is the charge, C_i is the concentration (mol m^{-3}), $\varphi$is the electrostatic potential (V), R is the gas constant (8.31 J mol^{-1} K^{-1}), T is the temperature (K) and v is the convective velocity along the X axis (m/s). Each term on the right hand side of Eq. (5) represents a specific mass transport mode: diffusion driven by the activity gradient, migration driven by the electrostatic potential gradient and convection due to the fluid motion, respectively:

$$\phi_i = \phi_{diff,i} + \phi_{mig,i} + \phi_{conv,i} \quad (6)$$

2.4.3. Ion transport in the bulk and transport number

In an MFC, steep activity gradients can occur in the vicinity of the electrode and separator surfaces. In contrast, in the bulk, far from the electrodes and separator, activity gradients are not so marked and, in absence of convection, the current is mainly driven by migration. Introducing the migration term into Eq. (4) gives the current density transported by each ionic species through the electrolyte, far from the separator and electrode surfaces:

$$J_i = J_{mig,i} = -{}_i C_i \frac{\partial \varphi(x)}{\partial x} \quad (7)$$

where λ_i is the molar ionic conductivity (m^2 S mol^{-1}) defined as:

$$\lambda_i = D_i z_i^2 \frac{F^2}{RT} \quad (8)$$

Values of λ_i are available in the literature. The λ_i value of a given species depends on the ionic composition of the electrolyte because interactions between ions alter the mobility of each ion. This is the reason why λ_i are often given for pure electrolytes and extrapolated to infinite dilution (Table 1). In some cases, ion mobility u_i (cm^2 V^{-1} s^{-1}) is given instead of λ_i, which is equivalent as ${}_{\lambda i} = z_i$ F u_i.

The current density passing through the reactor is the sum of the contributions of all species to ionic transport:

$$J = \sum_k J_k \quad (9)$$

so the part of the current that is transported through the electrolyte due to the motion of the ionic species *i* is given by:

$$t_i = \frac{J_{mig,i}}{J} = \frac{\lambda_i C_i}{\sum_k \lambda_k C_k} \quad (10)$$

and is called the transport number (or transference number) t_i. According to Eq. (9), the sum of the transport number of all the ionic species contained in an electrolyte is equal to unity:

Table 1
Molar ionic conductivities of cations λ_+^0 and anions λ_-^0 extrapolated to infinite dilution at 25 °C [83]. Some tables available in the literature give the equivalent ionic conductivities (m^2 S $equiv^{-1}$), which are equal to λ_i/z_i.

Cations	Molar ionic conductivity λ_+^0 (10^{-4} m^2 S mol^{-1})	Anions	Molar ionic conductivity λ_-^0 (10^{-4} m^2 S mol^{-1})
Ca^{2+}	118.9	CH_3COO^-	40.9
Cu^{2+}	107.2	Cl^-	76.3
Fe^{2+}	108	CO_3^{2-}	138.6
H^+	349.6	$HCOO^-$	54.6
K^+	73.5	HCO_3^-	44.5
Mg^{2+}	106	$H_2PO_4^-$	36
Na^+	50.1	HO^-	198
NH_4^+	73.5	HPO_4^{2-}	114
Zn^{2+}	105.6	SO_4^{2-}	160

$$\sum_k t_k = 1 \quad (11)$$

Finally, it should be mentioned that the denominator of Eq. (10) is the ionic conductivity, κ (S m^{-1} or Ω^{-1} m^{-1}), which measures the capacity of an electrolyte to ensure efficient ion transport:

$$\kappa = \sum_k \lambda_k C_k \quad (12)$$

Electrolytes can also be characterized by their ionic resistivity ρ (Ω m), defined as the inverse of conductivity. For a homogeneous electrolyte with a cross sectional area A, through which the current is transported over a distance *l*, the resistance to transport encountered by the ionic species (R_{tot}) is:

$$R_{tot} = \rho \frac{l}{A} = \frac{l}{\kappa A} \quad (13)$$

Applying Ohm's law, the ohmic loss (η_{ohmic}, V) due to the current flow through the electrolytes is:

$$\eta_{ohmic} = \frac{l}{\kappa} J \quad (14)$$

and the power density lost (P_{lost}, W m^{-2}) is:

$$P_{lost} = \frac{l}{\kappa} J^2 \quad (15)$$

Eq. (15) shows that the power consumed by ion transport through the electrolyte increases as the square of the current density, meaning that it is essential to tackle ion transport when the objective is to design a commercial MET able to operate at high current density.

2.4.4. How to use transport numbers and balance sheets

Transport numbers are very useful parameters which, in a straightforward manner, give the contribution of each ionic species to current carrying in conditions where migration is the dominant mode. Curiously, it has rarely been used in the context of MFCs, although this is a basic concept in electrochemistry and in membrane separation science. An objective of this article is to show how this parameter can be helpful in understanding, predicting, modelling and opening tracks for MFC development. Particularly, transport numbers can be very helpful to anticipate the behaviour of an MFC (or any other MER) from the simple analysis of the electrolyte.

On the basis of the electrolyte chemical composition, the transport number of each ionic species can be calculated using Eq. (10) with the molar ionic conductivities, which are reported in Table 1 for the most common ionic species contained in MFC electrolytes. These values correspond to infinite dilution and they should be corrected i to take the ionic interactions that occur in real solutions into account. Nevertheless, such a correction can be omitted for not too concentrated solutions. A simple and relevant way to assess the relevance of the theoretical approach is to calculate the ionic conductivity of the electrolyte through Eq. (12) and to compare it with the experimental measurement. It is advisable to take the opportunity of this calculation to check the charge balance of the electrolyte composition, because experimental data coming from raw analytical measures sometimes do not meet charge balance requirements (see comment in Section 3.4.5).

The transport numbers give the percentage of current that is transported by each species in the zones where migration is predominant, i.e. far from steep concentration gradients, in the absence of convection. This means in the bulk of the electrolyte, far from the electrode surface and far from the separator surface when there is one. Transport numbers thus give an immediate and accurate image of ion motion through the electrolyte. Another

way of representation this is to transform transport numbers into molar mass fluxes ($\phi_{mig,i}$) which are directly proportional:

$$\phi_{mig,i} = \frac{t_i}{z_i} \cdot \frac{J}{F} \quad (16)$$

The main difference is the charge z_i. The transport number, which gives the percentage of current transported, is directly proportional to the charge of the species. For instance, with identical molar fluxes, a divalent species transports twice as much current as a monovalent one.

Finally, close to the electrode surface, mass transfers are the sum of the migration and diffusion effects (absence of convection). Mass balance sheets can be calculated using Eq. (6). As a first approximation, it can be assumed that the transport numbers are identical in the bulk and in the diffusion layers near the electrodes. This hypothesis is fully valid if concentrations are high enough, so that only small changes in t_i are induced by the changes of local concentrations in the diffusion layers. The mass balance sheets give an accurate image of ion transport close to the surface of electrodes, which may be considered as essential if the objective is to characterize the electrode kinetics. The mass balance sheet indicates the actual operating conditions under which the electrode operates, which is very important information if the objective is to characterize or optimize the electrode kinetics.

Such a theoretical approach is illustrated in detail in Sections 3.4.1, 3.4.2 and 3.4.5 in the absence of separator and then recalled in Sections 5 and 6 for each type of ion-selective separator.

2.4.5. MFC performance assessment

The essential objective of an MFC is to produce power. The main performance criterion is consequently the maximum current or the maximum power produced. Current and power are extensive variables, which depend on the electrode surface, and performance is generally expressed as current density (J_{max}, A m^{-2}) or power density (P_{max}, W m^{-2}) with respect to the geometrical surface area of one of the electrodes. The two values are connected by the cell voltage (U_{cell}):

$$P_{max} = U_{cell} \cdot J_{max} \quad (17)$$

When three-dimensional electrodes are implemented, these values are expressed with respect to the volume of the electrode (A m^{-3}; W m^{-3}).

The MFC efficiency with respect to fuel consumption is measured by the Faradic yield, often called Coulombic efficiency (CE) in the MFC field. CE expresses the percentage (%) of the fuel that is actually transformed to electricity. CE is the ratio of the electrons that flowed through the electrical circuit during a given period of time (obtained by integrating the current) to the total amount of electrons that can be provided by the fuel consumed during the same period of time.

Several other criteria exist to assess MFC performance, particularly when the MFC has some other objective in addition to power production, such as effluent treatment, desalination, water reclamation, and biosensing. Nevertheless, the P_{max} or J_{max} and CE criteria are the most universal and the present review uses them as the basis for comparison.

3. Separator-less MFC

3.1. Why chemical gradients of fuel and oxygen are required in the electrolyte

Theoretically, both electrodes of a fuel cell could operate in exactly the same medium if each electrode was able to drive the reaction it is intended for. Selective electrodes, which are able to operate in this way, have been designed in enzymatic biofuel cells. Different enzymes are immobilized on the anode and cathode surfaces, which drive the electrode towards oxidation or reduction, respectively. For example, in enzymatic biofuel cells, the enzyme glucose oxidase wired on the anode surface and bilirubin oxidase or laccase immobilized on the cathode surface make both electrodes so selective that two electrodes can thus operate in the same electrolyte [84,85], fruit juice [86] or physiological fluids [87,88] for example, which contains uniform concentrations of both glucose and oxygen.

Unfortunately, similar selective electrodes are not available in the MFC field yet. As described in Sections 2.2.2 and 2.3.2, microbial anodes are very sensitive to the presence of oxygen and oxygen-reducing cathodes can be considerably disturbed by the presence of organic matter. To overcome these numerous detrimental effects, the anode must be immersed in an electrolyte that contains the fuel but no oxygen, while the cathode must be exposed to an environment rich in oxygen and free of fuel. Actually, no separator is required in between if the concentration gradients can be maintained between the anode and cathode zones.

3.2. Principle and limit of separator-less MFCs

Benthic MFCs are typical separator-less devices. The bioanode is immerged in anaerobic sediments rich in organic compounds and the cathode is in the overlying oxygenated seawater. The concentration gradients are maintained by taking advantage of the natural stratification of the water column caused by gravity [89,90]. Aerobic microorganisms that live in the intermediate zone between anode and cathode consume the dissolved oxygen and protect the bioanode from detrimental oxygen impact. The intermediate zone also prevents the organic compounds contained in the sediments from reaching the cathode.

In laboratory MFCs, a similar intermediate zone, in which fuel and oxygen are consumed by aerobic bacteria, also occurs between anode and cathode. This aerobic consumption of fuel can cause a considerable decrease in CE. Liu and Logan measured a CE around 40–55% in the presence of a separator that prevented oxygen from reaching the anode compartment, whereas the CE fell to 9–12% when the separator was removed [76].

In separator-less MFCs, the inter-electrode distance must be large enough to prevent oxygen from reaching the anode and the substrate from reaching the cathode. However, increasing the inter-electrode distance increases the ionic resistance (Eq. (13)) and consequently the ohmic drop (Eq. (14)) and the power density lost (Eq. (15)). This is not too much of a problem in benthic MFCs because they display low current densities and the ionic conductivity of marine sediments and seawater is high. The resulting ohmic drop remains low even with significant inter-electrode distance [91].

3.3. Interest of separator-less MFCs and how to develop them

Except in the specific case of benthic MFCs, which work in a saline electrolyte with modest current density, increasing the inter-electrode distance to ensure chemical gradients is a major hindrance for ion transport. Nevertheless, separator-less MFCs are not devoid of interest and have been widely used at the laboratory level [76,92,93]. Actually, using a separator between anode and cathode significantly increases the technical complexity of the device. It may require onerous maintenance for long-term industrial applications [94] and may be the source of a significant increase in the investment cost, particularly if membranes are implemented. The simplicity of separator-less MFCs is certainly an essential advantage that would deserve further development.

In our opinion, a clear distinction should be made between the interactions that can deactivate the electrode kinetics (Sections 2.2.2 and 2.3.2) and the parasite consumption of fuel and oxygen. The former must imperatively be avoided because they impact the essential function of an MFC. In contrast, parasite fuel consumption, which only results in decreased CE [95], may be not so detrimental for some applications, such as the treatment of effluents. When the most important target is to lower the level of an organic compound, for example, it can be accepted that some of the organic compound is not used to produce electricity but to ensure better operation of the MFC by ensuring the required chemical gradients between the anode and cathode. Thus, the necessity to sustain chemical gradients in the MFC would be paid for by the consumption of part of the fuel.

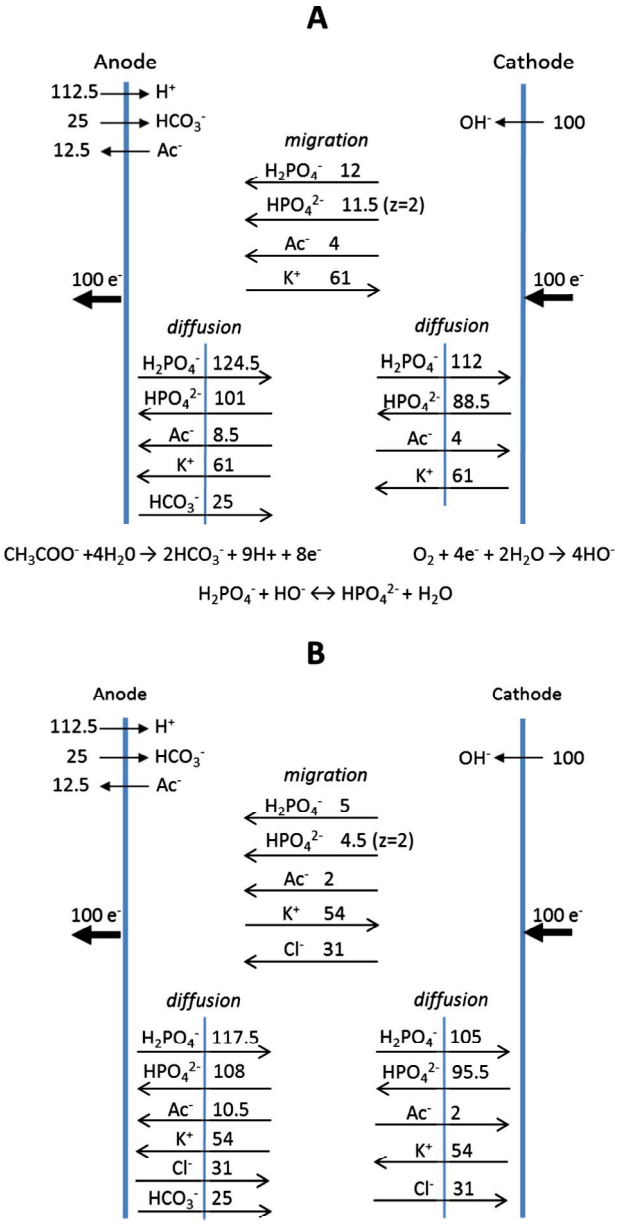

Fig. 2. Balance sheet without separator or with a non-selective separator. Molecular fluxes were calculated on the basis of 100 electrons exchanged per arbitrary unit of time. In the bulk, migration is assumed to be the dominant transport mode. Both migration and diffusion occur near the electrode surfaces. Transport numbers can be found in Table 2. (A) The electrolyte is composed of 50 mM phosphate buffer and 10 mM potassium acetate. (B) Same electrolyte with 100 mM KCl added.

Further development of separator-less MFCs should be aimed at controlling the zone where aerobic microorganisms consume oxygen and fuel. The simplest way would be to space the electrodes far enough apart to be sure that consumption of oxygen and/or fuel is completed. However, the larger the electrode spacing, the higher the internal resistance and ohmic drop (Eqs. (13) and (14)) [96,97].

To be more efficient, it may be possible to anchor the microorganisms to a highly porous intermediate structure (Fig. 3B). This porous structure would be technically less demanding than a conventional separator, because it would be solely intended to favour the development of an intermediate aerobic biofilm without strict sealing or other complex function. It would also introduce a smaller internal resistance because, with a largely open structure, the intermediate zone should have a conductivity close to that of the electrolyte. The objective would be to favour the development of an intermediate anaerobic biofilm achieving the chemical gradients of oxygen and fuel in a layer as narrow as possible. The intermediate aerobic biofilm would protect the bioanode against

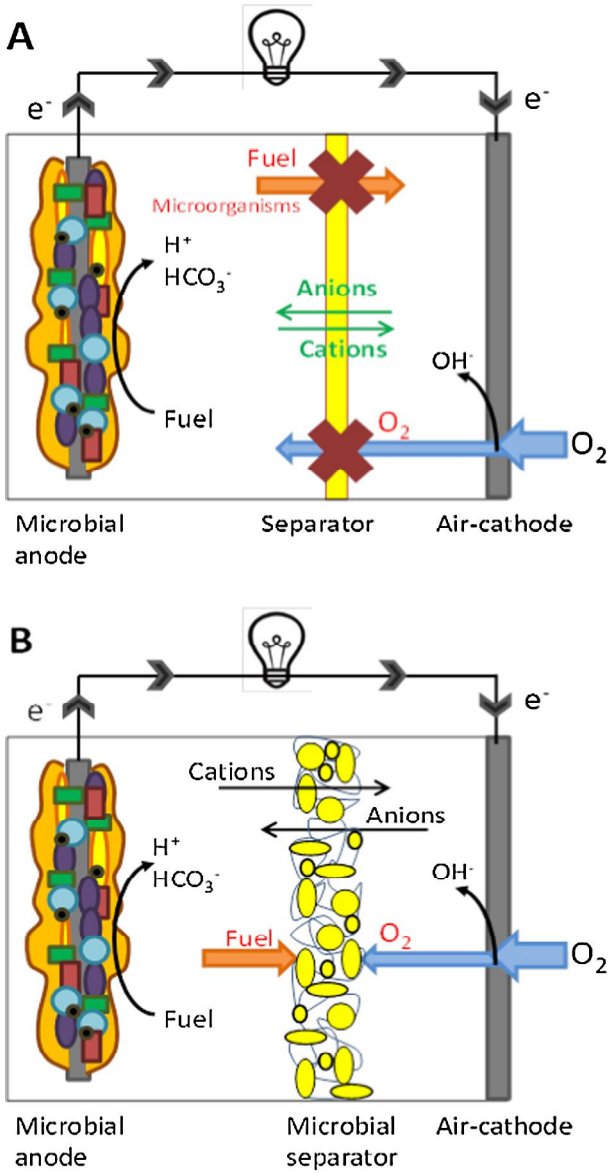

Fig. 3. Two-compartment air-cathode MFC. (A) The main functions of a separator should be to avoid oxygen transfer to the bioanode, to avoid fuel transfer to the cathode and to put up the smallest possible resistance to ion transfers. (B) These functions may also be ensured by an intermediate microbial layer implementing aerobic microorganisms, which would consume part of the fuel.

oxygen and the cathode against organic matter and the related inhibition effects (see Section 2.3.2). In most cases, the fuel flux should be greater than the oxygen flux, so it may be useful to provide this layer with oxygen. Investigating this new concept in depth would consequently lead researchers to reconsider the MFC design and operating procedure.

We propose that this concept be named "Microbial separator". Such a microbial separator has sometimes been observed to develop spontaneously in MFCs, for example in the form of an aerobic biofilm that grows on the cathode surface [80,98,99] or on the J-cloth used as a separator [100] (Section 6.5). Until now, microbial separators have formed spontaneously on surfaces that were not initially provided for this purpose. Nevertheless, the positive effect on MFC performance is observed. Dedicated research work should now aim at optimizing the support structure and its location inside the MFC, particularly by separating the microbial separator from the cathode surface to avoid the detrimental effect on OH^- mass transfer. It should be thus possible to gain considerable power production, at the price of fuel consumption.

3.4. Ion transport in separator-less MFC: numerical illustration

Current transport is illustrated with an electrolyte of pH 7.0 composed of 50 mM phosphate buffer and 10 mM potassium acetate, with or without addition of KCl, a medium commonly implemented in MFC laboratory experiments. This numerical illustration, proposed throughout the study, is made on the basis of a very simple medium, which is representative of a large number of MFC studies performed in laboratory conditions. The electrolyte is assumed to be quiescent and calculations are made on the basis of an initial state with uniform concentration of each species, as is the case when starting a batch cycle, for instance. The concentration of the anode product, e.g. HCO_3^- (Reaction (1)), is assumed to be nil.

3.4.1. Current transport in the bulk

The transport numbers (Table 2) show that current is mainly carried in the bulk by migration of K^+ ions towards the cathode (61%) and, to a lesser extent, by migration of phosphate ions to the anode (35%). Neither H^+ nor OH^- contributes to current carrying in the bulk. Contrary to what has too often been thought intuitively and by analogy with hydrogen fuel cells (Section 2.4.1), protons and hydroxide ions play absolutely no role in current carrying.

Table 2
Transport numbers in an electrolyte composed of 50 mM phosphate buffer and 10 mM potassium acetate, pH 7.0. Calculations were made with Eq. (10) with the equivalent ionic conductivities, λ_{0i}, extrapolated to infinite dilution (Table 1) without correction for concentrations. (A) The total ionic conductivity (κ) calculated with Eq. (12) was 0.95 S m^{-1}; (B) Same electrolyte with 100 mM KCl added; the total ionic conductivity was 2.45 S m^{-1}.

Species i	Concentration C_i (M)	$t_i \times 100$ (percentage)
(A) Phosphate 50 mM pH 7.0 and potassium acetate 10 mM		
H^+	10^{-7}	3.7×10^{-4}
OH^-	10^{-7}	2.1×10^{-4}
$H_2PO_4^-$	31×10^{-3}	12
HPO_4^{2-}	19×10^{-3}	23
CH_3COO^-	10×10^{-3}	4
K^+	79×10^{-3}	61
(B) Solution (A) with 100 mM KCl added		
H^+	10^{-7}	1.4×10^{-4}
OH^-	10^{-7}	8.1×10^{-5}
$H_2PO_4^-$	31×10^{-3}	5
HPO_4^{2-}	19×10^{-3}	9
CH_3COO^-	10×10^{-3}	2
K^+	179×10^{-3}	54
Cl^-	100×10^{-3}	31

This important conclusion can be demonstrated in a more general way. With a medium at pH 5, which can be considered as the acidic limit below which most microbial anodes are no longer able to operate, the conductivity due to protons ($\lambda_{H^+} \cdot C_{H^+}$) is equal to 3.5 10^{-4} S m^{-1} (λ_{H^+} in Table 1, $C_{H^+} = 10^{-2}$ mol m^{-3}). For protons to be responsible for more than 1% of the current transport through the bulk, the transport number t_{H^+} must be greater than 0.01. Eq. (10) indicates that, for the transport number of the proton to be higher than 1%, with $\lambda_{H^+} \cdot C_{H^+} = 3.5 \cdot 10^{-4}$ S m^{-1}, the conductivity of the medium (Eq. (12)) must be lower than 0.035 S m^{-1}. Consequently, protons do not contribute to current transport at pH equal to or higher than 5 for conductivity higher than 0.035 S m^{-1}. This value is very low, lower than in any electrolyte used in MFCs or other MERs so far, and it would preclude any efficient electrochemical process. It can be concluded that, for such time as acidophilic microbial anodes are not implemented, proton transport makes no contribution to current transport in the bulk of the electrolyte. An exception to this statement concerns osmotic MFCs. In this case, due to the massive rejection of all other ions, protons play the key role in current transport, but large scale development would be limited by the low concentration of protons (see Section 5.4.1) [101,102].

It should consequently be strongly recommended to abandon reasoning with proton transport in the bulk when the objective is to develop MFCs that operate around neutral pH. This way of thinking has already been adopted by several research groups [40,65,78,103,104] but a large number of studies still aim at improving the proton transfer capability of proton exchange membranes with the objective of improving MFC power production. The large number of recent studies in this direction [105–109] incited to stress this issue here.

The mass transfer balance sheet presented in Fig. 2A was achieved on the basis of 100 electrons exchanged through the external circuit per arbitrary unit of time. The molecular fluxes corresponding to 100 electrons exchanged per unit of time were calculated from the transport number according to Eq. (16).

3.4.2. Balance sheet close to the electrode surfaces and buffering

Close to the surface of the electrodes, concentration gradients are created by the electrochemical reactions and diffusion significantly impacts the mass transfer balance. In the absence of convection, each mass flux is the sum of the diffusion and the migration contributions (Eq. (6)). It was assumed here that the transport numbers were identical in the bulk and in the diffusion layers near the electrodes. This hypothesis is valid if concentrations are high, so that only small changes in t_i are induced by the changes of local concentrations in the diffusion layers.

The cathode provided with oxygen and water produced 100 OH^- ions per unit of time (Reaction (3)). For the sake of simplicity, the acid-base equilibrium of the phosphate species was assumed to be instantaneous:

$$H_2PO_4^- \leftrightarrow HPO_4^{2-} + H^+ \quad (18)$$

and the possible involvement of the HCO_3^- ions was not taken into account in the acid-base balance, so the 100 OH^- ions produced roughly resulted in the consumption of 100 $H_2PO_4^-$ and the production of 100 HPO_4^{2-}. According to the values of the transport numbers, migration expelled 12 $H_2PO_4^-$ and 11.5 HPO_4^{2-} ions from the cathode surface. Consequently, to maintain the steady state, diffusion had to provide the electrode with 112 $H_2PO_4^-$ and to remove only 88.5 HPO_4^{2-} ions. Near the cathode surface, the diffusion and migration fluxes of the $H_2PO_4^-$ ions are opposite, while diffusion and migration cooperate to remove the HPO_4^{2-} ions produced. The ions whose concentration is not affected by the electrochemical reaction (e.g. Ac^- and K^+ on the cathode surface) must have a nil balance sheet, and diffusion must compensate the effect of migration.

At the anode, to sustain the steady state with 100 electrons extracted per unit of time, 12.5 acetate molecules must be supplied to the anode (Reaction (1)). Only 4 acetate molecules are provided by migration. An additional 8 acetate molecules must be supplied by diffusion. Besides, 25 HCO_3^- and 112.5 H^+ are produced per unit time by acetate oxidation (Reaction (1)). The balance on phosphate ions is done in the same manner as for the cathode. In this case, migration hinders the motion of the $H_2PO_4^-$ ions away from the anode, which must be compensated by diffusion.

The balance sheet shows that buffering is mainly ensured by diffusion of the phosphate species near the surface of the electrodes. Migration has only a slight effect on buffering. Actually, by moving $H_2PO_4^-$ from the cathode towards the anode, migration makes a detrimental contribution to the buffer effect which, on the contrary, requires $H_2PO_4^-$ to be driven away from the anode towards the cathode.

3.4.3. Effect of adding a supporting salt (Table 2B, Fig. 2B)

If 100 mM KCl is added into the electrolyte, migration of K^+ always makes the main contribution to current transport in the bulk (54%). The contribution of the phosphate ion migration is reduced to 14% because migration of Cl^- takes charge of 31% of the current transport. As can be expected, the supporting salt ensures a significant part of current transport in the bulk and reduces the contribution of the other ionic species. This can also be seen by calculating the ionic conductivity, which is significantly increased from 0.95 to 2.45 S m^{-1} by the addition of 100 mM KCl. The ohmic drop should thus be divided by a factor greater than 2.

The balances drawn up close to the electrode surfaces (Fig. 2B) give similar mass fluxes to the previous ones. The negative/positive effects of migration of the phosphate species on buffering are attenuated, as can be expected when adding a supporting salt.

3.4.4. Evolution of pH and ionic concentrations in an MFC during operation

In an operating MFC, the pH decreases near the anode (Reaction (1)), while it increases near the cathode (Reaction (2)). This phenomenon has often been confirmed experimentally [103,110,111]. The numerical illustration calculated with the initial concentrations of the buffering species showed that, in the bulk, migration moves both $H_2PO_4^-$ and HPO_4^{2-} ions towards the anode with approximately equal molecular fluxes. On the basis of 100 electrons passing through the system, the conditions considered in Fig. 2A led to 12 and 11.5 molecules of $H_2PO_4^-$ and HPO_4^{2-} respectively. Only 11.5 molecules of HPO_4^{2-} are carried by migration to the anode, while 112.5 protons are produced. Migration cannot efficiently mitigate anode acidification. Diffusion of HPO_4^{2-} must contribute strongly to pH balance, but diffusion is not a fast process and is not proportional to the current density. Consequently, the local acidification of the anode biofilm is moderately mitigated by migration of buffering species and is strongly dependent on diffusion. This would become a major hindrance if the objective is to provide high current density.

This situation is even aggravated by the addition of 100 mM KCl (Fig. 2B). In this case only 4.5 molecules of $H_2PO_4^-$ are moved towards the anode by migration. Adding a supporting salt improves the global ion transport and decreases the ohmic drop but, in return, it decreases the capacity of the bulk to fight against anode acidification.

One way to enhance pH balance inside the cell would be to create convective mass transport by stirring or circulating the electrolyte [39]. Nevertheless, it should be kept in mind that stirring or circulating costs energy, more energy than the MFC could produce as the state of the art stands at the moment. This solution may be suitable only for specific cases.

This situation with phosphate occurs because, around neutral pH, the two species involved in buffering are negatively charged ($H_2PO_4^-$ and HPO_4^{2-}, reaction (17)). They are both driven towards the anode by migration. A different pattern would be found if a form of the buffer was not charged:

$$AH \leftrightarrow A^- + H^+ \quad (19)$$

In this case, only the alkaline form (A^-) is driven by migration towards the anode, which should result in a better mitigation of bioanode acidification.

For the same reason, Logan's group has recently shown that positively-charged non-dissociated buffers (AH^+):

$$AH^+ \leftrightarrow A + H^+ \quad (20)$$

are more efficient than non-charged or negatively-charged buffers to mitigate alkalinization of oxygen-reducing cathodes (Reaction (3)) [112]. Obviously, a positively-charged buffer would not be suitable for controlling the bioanode pH, but a multi-species buffer may be envisioned, including a non-charged compound and a positively-charged compound to optimally mitigate both bioanode acidification and cathode alkalinization.

The pH balance inside MFCs, or any other MER, is a major source of current limitation. When the objective is to maximize the power produced by MFCs, this issue definitely deserves dedicated studies. In this context, transport numbers in the bulk and balance sheets at the surface of electrodes would be the essential theoretical tools to optimize ion transport for pH balance. Experimental validation of the theoretical prediction is then required, at least to check whether the microorganisms accept the nature and concentration of the buffers.

3.4.5. Numerical illustration with wastewater used as electrolyte

This review does not intend to review all the possible MFC electrolytes but aims at developing a general theoretical rationale that can then be used for other cases. The numerical illustration made throughout the study with a phosphate buffer solution, supplemented or not with KCl, corresponds to the majority of laboratory studies reported so far. An additional short numerical illustration is given here relating to the field of wastewater treatment, a possible application domain for MFCs (Table 3). The transport numbers were calculated as previously with Eq. (10) from the data gathered in Table 1.

The majority of the electricity (35.9%) was carried through the electrolyte by the movement of Cl^- ions. This example confirms that the capacity of migration to mitigate bioanode acidification depends on the pH of the bulk. In this case, migration drove a larger amount of HPO_4^{2-} than $H_2PO_4^-$ towards the anode, which is an advantage to attenuate the anode acidification. Nevertheless, the transport numbers show that pH balance will be modest as only

Table 3
Transport numbers in an electrolyte composed of wastewater. The ionic composition was extracted from Le Bonté et al. [113], with a pH value averaging 7.8. Calculations were made using Eq. (10) with the equivalent ionic conductivities, λ_{0i}, extrapolated to infinite dilution (Table 1) without correction for concentrations.

Species i	Concentration C_i (M)	$t_i \times 100$ (percentage)
H^+	1.6×10^{-8}	4.1×10^{-4}
OH^-	6.3×10^{-7}	9.2×10^{-3}
Ca^{2+}	2.1×10^{-3}	18.5
K^+	0.26×10^{-3}	1.4
Mg^{2+}	0.33×10^{-3}	2.6
Na^+	3.1×10^{-3}	11.5
NH_4^+	1.8×10^{-3}	9.8
Cl^-	6.34×10^{-3}	35.9
$H_2PO_4^-$	0.08×10^{-3}	0.2
HPO_4^{2-}	0.37×10^{-3}	3.1
SO_4^{2-}	1.42×10^{-3}	16.9

3.1% of the current was transported by the HPO_4^{2-} ions. In return, migration was less effective in expelling negative charges from the cathode zone. This is a strong disadvantage here because of the quantities of Ca^{2+} ions contained in wastewaters. The Ca^{2+} ions carried a considerable proportion of the electricity (18.5%) by moving to the cathode. The poor efficiency of phosphate species in balancing the pH of the cathode zone and the large flux of Ca^{2+} ions converge to predict fast cathode fouling because of the formation of scale. This illustration shows how transport numbers can help to predict some aspects of MFC behaviour from the simple analysis of the electrolyte composition.

From a practical point of view, looking for data to present this numerical illustration, pointed out the difficulty to obtain an exhaustive list of the ionic contents of wastewaters; often, the existing data were not balanced from the point of view of charges. In the present case, it was necessary to multiply by a factor of 1.67 the anion concentrations reported in the article to reconcile the experimental data with charge balance. The calculated ionic conductivity, κ, of 0.13 S m^{-1} was consistent with the average experimental value of 0.11 S m^{-1}. In the context of MFC development for wastewater treatment, and given the great impact of ion transport on MFC behaviour, preliminary analytical work to determine the ionic composition of wastewaters would be most helpful.

4. Functions of a separator in MFC

4.1. The ideal separator and even more

The role of the separator is to overcome the lack of selectivity of the electrodes used in MFCs. It must allow two zones with different chemical compositions to be maintained inside an inter-electrode space that is as narrow as possible. Basically, an ideal MFC separator designed for maximizing power production would (Fig. 3A):

(1) prohibit the transfer of oxygen to the anode,
(2) prohibit the transfer of the fuel and other organic matter to the cathode,
(3) not introduce any resistance to the transfer of ionic species.

In practice, it should not be forgotten that a separator cannot fully validate condition 3. In all cases, a separator introduces resistance to the mass transfer for each species, including ions. It is essential to keep in mind that any separator introduces additional resistance to ion transport. According to Eqs. (14) and (15), the function of a separator is to maintain chemical gradients while reducing the distance l to a minimum and keeping a reasonable value of κ inside the separator.

Many separators are able to modulate the resistance to mass transfer according to the size and/or the charge of the compounds. Thanks to the capacity of these separators to impact ion transports, additional functions can be attributed to them. For example, they could also:

(4) protect the cathode against (bio-)fouling,
(5) allow the MFC target to be enlarged far beyond the simple production of electricity. This is typically the case with ion-exchange membranes, which push the MFC towards specific operational strategies. MFC devices have thus been designed for water desalination [114–116], selective removal of ions [117], reverse electrodialysis [118,119], effluent denitrification [120,121], ammonium recovery [122,123], effluent treatment by alkalization [124], etc. Osmosis membranes can also be implemented to add a water reclamation objective [101] (see Section 5.4). Such specific functions would deserve a dedicated theoretical approach, which is beyond the scope of the present article.

Depending on the nature of the cathode, the main purpose assigned to the MFC (to optimize power density, to increase CE, to maximize an effluent treatment, to abate the concentration of a given compound, etc.), or the type of process that may be associated with the MFC, many configurations have been reported to implement separators in MFCs. The different MFC designs have been reviewed elsewhere [31,125,126] and are not detailed here. It can just be recalled that the most recent configurations include a separator-electrode assembly (also called membrane-electrode assembly), in which the separator is sandwiched between the anode and the cathode [127,128]. This technology should be a very promising way to reduce the ohmic drop by reducing the inter-electrode distance to its minimum.

4.2. Separator characteristics and classification

The literature reports a wide diversity of separators tested in MFCs. They can be divided into two major categories: non-porous and porous separators. Table 4 gives a basic classification

Table 4
Separator classification according to the membrane type, the pore diameter and the rejected species. From [129,130].

	Ion Exchange Membrane (IEM)			Reverse and Forward Osmosis (RO / FO)	Nano-Filtration (NF)	Ultra-Filtration (UF)	Micro-Filtration (MF)	Macro-Filtration
	Cation Exchange Membrane (CEM)	Anion Exchange Membrane (AEM)	Bipolar Membrane (BPM)					
Type	Non porous				Porous			
	Ion-selective			Non ion-selective	Ion-selective	Non ion-selective		
Pore diameter (Å)	/				10-100	100-1000	1000-10^4	> 10^4
MWCO (Da)	/				250-2000	2000-500,000	/	
Smallest rejected species	Atoms			Monovalent and divalent ions	Small particles, Sugars, Aqueous salts	Proteins, Polysaccharides, Viruses	Solids, Bacteria	Macro-particles, Colloids, Granules
Observation technique	Transmission Electron Microscopy				Scanning Electron Microscopy		Optical microscopy	Naked eye

ranging from the most compact non-porous membranes to the most porous separators. Following this classification, each type is analysed thereafter with respect to its impact on ion transport.

5. Non-porous separators

Table 5 gathers together the characteristics of non-porous separators used in MFCs so far. As it is crucial to prohibit oxygen transfer to the bioanodes, many studies have focused on oxygen diffusion through the membranes, with pretty dispersed results. A quick glance at this table gives an idea of the difficulty of extracting firm, universal conclusions from experimental studies carried out with different experimental set-ups, different microbial systems and different conditions. Nevertheless, an attempt is made here to analyse these experimental data in the light of the theory.

5.1. Cation exchange membrane (CEM)

Cation exchange membranes (CEMs) contain negatively charged groups, such as $-SO_3^-$, $-COO^-$, $-PO_3^{2-}$ or $-PO_3H^-$, fixed to the membrane backbone, which gives them a selective permeability for cations [144]. CEMs include proton exchange membranes (PEMs), which are specially designed to allow proton transfer and to oppose a high resistance to the transfer of all other ions.

5.1.1. Basics on ion transport controlled by CEM

Theory indicates that protons are not involved in current carrying in MFCs (Section 3.3). Consequently, the use of a PEM in an MFC can hardly be justified except if microbial anodes could operate at very low pH. Unfortunately, to our knowledge, acidophilic bioanodes still remain poorly developed [47,145,146] and it remains a worthwhile challenge to develop such efficient bioanodes. Much work has been carried out to improve the proton exchange capacity of PEMs [105,107] [108,109], with some successes in terms of MFC performance [147]. Nevertheless, the objectives and results should not be discussed in terms of proton transfer, when improvement was related to the transfer of other cations present in solution (K^+, Na^+, Mg^{2+}, Ca^{2+}, etc.) as confirmed experimentally [103,111,133].

The buffer ionic species $H_2PO_4^-$ and HPO_4^{2-} are strongly retained by a CEM. By prohibiting the diffusion of the buffer ionic species between the anode and cathode compartments, a CEM severely hinders the pH balance in an MFC implemented with phosphate buffer. The balance sheet calculated in the presence of a CEM (Fig. 4) shows that the whole current results from the motion of the K^+ ions. If KCl is added as a supporting salt, part of this desirable action is lost because the Cl^- ions cannot take part in the current transport. The balance sheet also demonstrates that the anode compartment tends to be deionized, while the ionic concentration of the cathode compartment increases.

In long-term operation, complex ion transport situations can occur. Electro-osmosis, due to the transport of the water molecules that compose the K^+ solvation layer [148,149] should be taken into account. Ultimately, the K^+ concentration gradient will drive a backward diffusion flux that will oppose migration and hinder MFC operation. The gradient in water activity caused by K^+ migration may also lead to the diffusion of water from the anode to the cathode compartment by osmosis. The long-term ion transport would deserve a dedicated analysis, with the same theoretical tools as used here, by taking the modification of the chemical composition in each compartment into account.

Basic analysis of ion transport points out numerous drawbacks that make it hard to justify using a CEM in an MFC, except for specific cases. For instance, the CEM can ensure the function of fuel retention in the anode compartment perfectly when the fuel is in anionic form (see Section 5.2.2). If saving fuel is seen as essential, using a CEM may be justified. Similarly, when the objective is to couple power generation with another function, such as desalination [114,116] or other kinds of separation processes (34), CEM can also be fully relevant. The balance sheet (Fig. 3) shows that cations can easily be extracted from the electrolyte, which may be essential when a separation function is assigned to the MFC (see point 5 in Section 4.1). Nevertheless, except in such specific cases, which deserve a dedicated theoretical analysis, blocking the motion of anions by a CEM is a major drawback for conventional MFCs.

5.1.2. CEM in the MFC literature

Among CEMs, PEMs have been particularly used in MFCs, probably by analogy with PEMFCs. Nafion membranes from Dupont are the most commonly used PEMs. They offer high proton conductivity due to sulfonate groups fixed on an inert backbone (PTFE-like skeleton) [134]. They are classified according to their molecular weight cut-off and nominal thickness [150]. For example, the numbers "11" and "7" in Nafion 117 refer to 1100 g "equivalent weight" and 7/1000 in., respectively, where the equivalent weight defines the weight of Nafion in molecular mass per sulfonic acid group. Similarly, Nafion 112 and Nafion 115 are 2/1000 and 5/1000 in. thick, respectively.

Rahimnejad et al. 2010 observed that the thinner Nafion 112 led to better performance than Nafion 117 [151]. In contrast, Ghasemi et al. measured a considerably lower power production with Nafion 112 than with Nafion 117 (19.7 mW m^{-2} against 126.1 mW m^{-2}) and assumed that it was due to the greater diffusion of oxygen to the bioanode with Nafion 112 [152]. This discrepancy illustrates the difficulty of establishing universal conclusions, probably because of the great dependence of the results on the experimental set-ups and operating conditions.

A wide range of values have been reported for the oxygen mass transfer coefficient in Nafion 117: 1.3×10^{-4} cm s^{-1} by Kim et al. [133] or 2.80×10^{-4} cm s^{-1} by Chae et al. [134], while Khilari et al. [135] measured only 2.8×10^{-5} cm s^{-1}. Here again, the differences in the experimental set-ups (two-compartment MFC with an immersed cathode for the first two, single-compartment MFC with an air cathode for the last) or in electrolyte compositions might have been sources of discrepancy. Nevertheless, in our opinion, such significant oxygen transfer rates through Nafion membranes are surprising, as these membranes were designed to separate O_2 and H_2 under high pressures in PEMFC. The hypothesis of a different mechanism of O_2 crossover in aqueous conditions cannot be discarded, neither can possible oxygen leakages in the experimental set-up disturbing the measurements. If PEM is judged to be justified for a specific MFC, this issue should be tackled in priority.

Because Nafion remains one of the most expensive PEM (approx. \$1400/m^2) low-cost alternatives have been investigated [153,154]. Among them, the Ultrex membrane (CMI 7000, Membrane Inc., USA) has been widely tested in MFCs [133]. It is a strong acid CEM composed of a polystyrene gel cross-linked with divinylbenzene that contains sulfonic acid groups. Compared in identical conditions, it presented a higher ionic resistance (45 Ω cm^{-2}) than Nafion 117 (9.2 Ω cm^{-2}) due to its greater thickness (457 vs. 183 μm for Nafion 117) [132].

Although trying to increase the proton transfer rate through PEM in order to enhance MFC performance is a theoretical impasse, many studies have been devoted to PEM modifications. They are overviewed in Table 6.

PEMs are affected by fouling and biofouling during long-term operation, which can significantly reduce their ion exchange capacity [155,156]. Removing the biofouling layer may not be suf-

Table 5
Characteristics of non-porous membranes reported in the MFC literature. Both manufacturer's data and parameters calculated from experimental data, such as mass transfer coefficients, are given. Manufacturer's data are indicated by an asterisk ∗.

Membrane	Composition	Thickness (mm)	Ohmic resistance (Ω cm^2)	Oxygen mass transfer k_O (cm s^{-1})	Oxygen diffusion coefficient D_O (cm^2 s^{-1})	Acetate mass transfer k_A (cm s^{-1})	Acetate diffusion coefficient D_A (cm^2 s^{-1})	Ion exchange capacity (meq g^{-1})
Cation exchange membranes (CEM)								
Nafion 117, Dupont Co., USA	Chemically stabilized perfluoro-sulfonic acid/PTFE copolymer in the acid form negatively charged sulfonate groups	183*	15 in 0.5 M NaCl* 1.5 [131] 9.2 in 0.05 M K_2HPO_4/KH_2PO_4 [132]	1.3×10^{-4} [133] 2.8×10^{-4} [134] 2.8×10^{-5} [135] 8×10^{-5} [136] 0.3×10^{-4} [137] 4.3×10^{-4} [138] 7.5×10^{-5} [139]	2.4×10^{-6} [133] 5.35×10^{-6} [134] 4.2×10^{-7} [135] 0.55×10^{-6} [137] 8.2×10^{-6} [138] 1.4×10^{-6} [139]	4.3×10^{-8} [133]	0.82×10^{-9} [133]	0.95 to 1.01* 1.23 [136]
CMI 7000, Membrane Inc., USA	Gel polystyrene cross linked with divinyl-benzene, sulfonic acid groups	450*	<30 in 0.5 M NaCl* 45.1 in 0.05 M K_2HPO_4/KH_2PO_4 [132]	0.94×10^{-4} [133] 0.1×10^{-4} [138] 2×10^{-5} [139]	4.3×10^{-6} [133] 9.8×10^{-6} [138] 0.9×10^{-6} [139]	1.4×10^{-8} [133]	0.66×10^{-9} [133]	1.6*
SPEEK	Sulfonated poly(ether ether ketone)	180 [136]			4×10^{-6} [136]			1.47 [136]
SPEEK + 7.5% TiO_2	Modified SPEEK membranes by incorpo-rating TiO_2	180 [136]			2.2×10^{-6} [136]			1.98 [136]
SPEEK + 7.5% SiO_2	Modified SPEEK membranes by incorpo-rating SiO_2	120 [140]			0.84×10^{-6} [140]			1.80 [140]
Anion exchange membranes (AEM)								
AMI-7001, Membrane International Inc., NJ	Gel polystyrene cross linked with divinyl-benzene, quaternary ammonium groups	460*	<40 in 0.5 M NaCl*	0.94×10^{-4} [133] 1.6×10^{-4} [141] 0.1×10^{-5} [142]	4.3×10^{-6} [133] 3.1×10^{-7} [141] 3×10^{-7} [142]	5.5×10^{-8} [133] 4.6×10^{-8} [141] 4.7×10^{-8} [142]	2.6×10^{-9} [133]	1.3*
Ralex AEM-PES, MEGA a.s., Czech Republic	Polyester with poly-ethylene binder quaternary ammonium group	450 (dry)* 750 (swelled)*	<7.5 in 0.5 M NaCl*					1.8 [131]
AFN, Tokuyama Co., Japan	Quaternary ammonium group	150–180 [131]	0.2–1 in 0.5 M NaCl [131]	1.26×10^{-4} [143]	1.9×10^{-6} [143]			3.2* 2–3.5 [131]
AM1, Tokuyama Co., Japan		120–160 [131]	1.3–2 in 0.5 M NaCl [131]	0.98×10^{-4} [143]	1.4×10^{-6} [143]			1.8–2.2 [131]
ACS, Tokuyama Co., Japan		120–200 [131]	3–6 in 0.5 M NaCl [131]	0.65×10^{-4} [143]	1.2×10^{-6} [143]			1.4–2 [131]
FAD, Fumasep	Poly(ether ether ketone) (PEEK) reinforced and non-reinforced films	80–100*	<1 in 0.5 M NaCl* 1.2 [131] 12.4 in 0.05 M K_2HPO_4/KH_2PO_4 [132]					>1.5* 1.3 [131]
QPEEK-AEM	AEM quaternized PEEK	0.2 [141]		2.1×10^{-4} [141]	4.8×10^{-8} [141]	5.2×10^{-8} [141]		1.39 [141]
LeHoAM-III Hangzhou Lvhe Environmental Technology Co., Ltd., China		240 [137]		0.05×10^{-4} [137]	0.11×10^{-6} [137]			
TiO_2-QAPVA hybrid AEM	Organic-inorganic hybrid AEM synthesized with quaternized poly(vinyl alcohol) (QAPVA) and inorganic TiO_2	43 [137]		0.05×10^{-4} [137]	0.02×10^{-6} [137]			
QPEI-AEM	AEM-quaternized poly(ether imide)	0.03 [142]		2.3×10^{-5} [142]	4.7×10^{-7} [142]	4×10^{-8} [142]		0.968 [142]
Bipolar membrane (BPM)								
FBM, Fumasep	Mechanical reinforcement SPEEK monofil	180*	<3 in 0.5 M NaCl*					

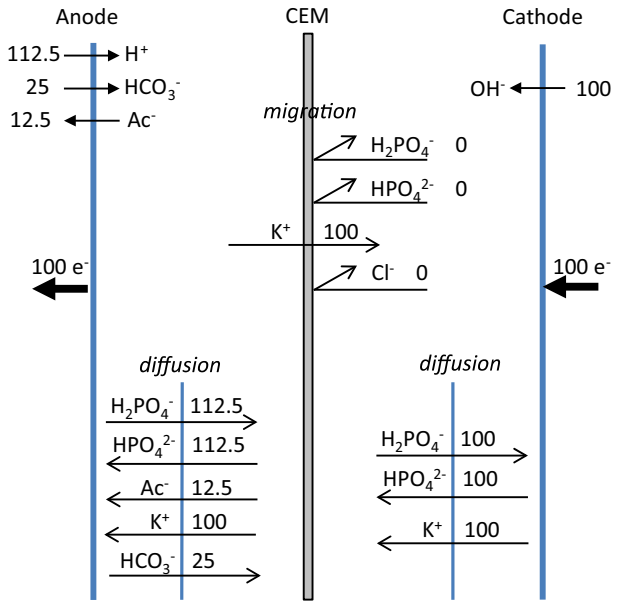

Fig. 4. Balance sheet of the molecular fluxes with a cation exchange membrane (CEM). The electrolyte is composed of 50 mM phosphate buffer and 10 mM potassium acetate. It is assumed that no acetate was initially put into the cathode compartment.

ficient to recover the initial characteristics and it may be necessary to regenerate the CEM functional groups [157]. The resistance to biofouling has been enhanced for some composite CEMs by increasing the proportion of a given compound: GO for GO-PVA-STA membranes [135] or polyaniline for Nafion/PANI composite membranes [158].

5.2. Anion exchange membrane (AEM)

Anion Exchange Membranes (AEMs) have a selective permeability for anions due to the positively charged groups they contain, covalently bound to their polymer backbone [37,144]. Anion exchange functional groups can be either strongly basic, such as tertiary ammonium, or weakly basic, such as primary, secondary or tertiary amine groups [131]. The wide use of AEMs in all types of fuel cells, including MFCs, has recently been detailed in a comprehensive review [37]. AEMs have been less often reported in MFC studies than CEMs but with a significant diversity of types (Table 5).

5.2.1. Advantages of AEM vs. CEM

AEMs allow anions to pass through. The theoretical balance sheet (Fig. 5) shows that this is a great advantage over CEMs for MFCs, because AEMs introduce a smaller resistance to the pH balance role of the $H_2PO_4^-$ and HPO_4^{2-} species. AEM creates minimum hindrance to the pH balance by anionic species between the two compartments.

This advantage has often been confirmed experimentally [165,166], particularly the virtuous association with phosphate or bicarbonate buffer [40,167,168]. Compared in a two-compartment MFC, an AEM produced a larger power density (610 mW m^{-2} with AMI-7001 from Membrane International Inc., NJ) than CEMs (514 mW m^{-2} with Nafion; 480 mW m^{-2} with CMI-7000 from Membrane International Inc., NJ), or an ultrafiltration membrane (462 mW m^{-2}) [133]. The better suitability of AEM than CEM or ultrafiltration membrane was also observed when the membrane was used to support an oxygen-reduction cathode. One side of the membrane was made conductive using graphite paint and a non-precious metal catalyst to form a membrane-cathode configuration [168]. AEM has also proved more appropriate than PEM in the design of a membrane-electrode assembly [169]. Similarly to CEM a few studies have been aimed at designing specific AEM for MFCs (Table 6).

A lower oxygen mass transfer coefficient has also been measured for AEM than Nafion (0.94×10^{-4} cm s^{-1} and 1.3×10^{-4} cm s^{-1} respectively) [133]. Nevertheless, a large range of values have been reported in the MFC literature. For instance, Ji et al. have measured oxygen transfer coefficients from 0.65×10^{-4} cm s^{-1} to 1.26×10^{-4} cm s^{-1} for three different commercially available AEMs (ASTOM Co., Yamaguchi, Japan) [143]. As mentioned above for CEMs, it is difficult to make relevant comparisons on this issue.

Finally, comparing the balance sheets of CEM (Fig. 4) and AEM (Fig. 5) shows that CEM favours the access of cations to the cathode, while AEM hinders it. AEM should consequently mitigate cathode fouling due to alkaline precipitation (Section 2.2). This advantage has also been noted experimentally [169,170]. An antibacterial effect of QAPVA/TiO_2 membrane has also been noted as positive [137].

5.2.2. In a few circumstances AEM perform less well than CEM

AEM may have some disadvantages compared to CEM when the fuel used is in anionic form, e.g. the widely used volatile fatty acids (acetate, propionate, butyrate, etc.). If the fuel is fed into the anode compartment only, migration through an AEM can only weakly oppose the diffusion-driven flux established from the anode to the cathode compartment. The diffusion flux from anode to cathode would form a countercurrent to migration (see balance sheet Fig. 5), in opposition to current carrying. Some of the anionic fuel is unavoidably lost with AEM, and feeding only the anode compartment would lead to detrimental diffusional flux. As described in Section 2.4, the access of the fuel to the cathode compartment has detrimental effects, which have been confirmed experimentally [133,143,166].

AEMs have proved to be more subject to membrane deformation. Zhang et al. found that the performance of a single-compartment MFC equipped with a membrane pressed against the air-cathode was reduced when an AEM was used (AMI-7001 from Membrane International Inc.) rather than a CEM (CMI-7000) (16 ± 2 W m^{-3} vs. 21 ± 2 W m^{-3}, respectively) [170]. This difference was attributed to membrane swelling during ion transport through the membrane, which induced detrimental deformation of the AEM.

5.3. Bipolar membrane (BPM)

A BPM is composed of a cation exchange layer and an anion exchange layer mounted together to form a humid junction interface. The humid interface between the two layers is generally considered as a third layer. Under the effect of an electric field, the water content of the membrane is split into protons and hydroxide ions. Protons and hydroxide ions respectively migrate through the CEM, which faces the cathode compartment, and through the AEM, which faces the anode compartment. BPM would consequently be able to stabilize the pH in both compartments of an MFC by supplying the cathode compartment with protons and the anode compartment with the same amount of OH^- ions. The theory, already presented elsewhere [40], is not described in detail here. BPM offers an apparently very appealing solution to the thorny problem of pH gradient in MFCs. Unfortunately, water splitting requires a lot of energy, which is deducted from the power supplied by the MFC and BPM would heavily burden the energy balance. The few existing experimental achievements implemented more efficient cathode reaction than oxygen reduction [171,172].

Table 6
Performance of various advanced laboratory-made CEMs and AEMs designed for MFC.

Nature	MFC performance	Comment	Ref.
CEM: Modified Nafion			
Nafion 112-polyaniline composite (Nafion/PANI)	124 mW m^{-2}, around nine fold power density obtained with Nafion 112		[158]
Supported ionic liquid Nafion	215 mW m^{-2} vs. 157.9 and 102.2 mW m^{-2} with Nafion 117 and Ultrex CMI-7000, respectively		[109]
Nafion 117 reinforced with PVA	Up to 91 mW m^{-2} vs. 79 mW m^{-2} with Nafion 117		[159]
CEM: Alternative membranes to Nafion			
SPEEK	77.3 mW m^{-2} vs. 106.7 mW m^{-2} with Nafion 117	Power production with SPEEK was lower than with Nafion 117 but SPEEK was assessed to be about twice as cost effective because of its lower price	[160]
	126.1 mW m^{-2} vs. 179.7 mW m^{-2} with Nafion 117		[161]
GO-PVA-STA	86.7 mW m^{-2} vs. 64.5 mW m^{-2} with Nafion 117	Oxygen mass transfer coefficient of 6.1×10^{-6} cm s^{-1} was lower than that of Nafion 117 of 2.8×10^{-5} cm s^{-1}	[135]
Composite GO-SPEEK	902 mW m^{-2} vs. 1013 mW m^{-2} with Nafion 117 and 812 mW m^{-2} with a non-modified SPEEK membrane	Nafion 117 produced the highest power density and GO-SPEEK had the highest O_2 diffusion coefficient (1.15 10^{-6} cm^2 s^{-1}) but GO-SPEEK is less expensive	[106]
Nanofibre-reinforced composite based on SPEEK		Lower fuel crossover compared to Nafion	[159]
Carbon nanocomposite	57.6 mW m^{-2} vs. 14.0 mW m^{-2} with Nafion 112		[162]
Modified SPEEK membranes by incorporating TiO_2 or SiO_2	98.1 and 1008 mW m^{-2} with TiO_2 and SiO_2, respectively; higher performance than with SPEEK and Nafion 117	Oxygen mass transfer coefficient decreased with the increase in TiO_2 or SiO_2, up to 2.2×10^{-6} and 0.7×10^{-6} cm s^{-1} respectively	[136,140]
Modified SSEBS membrane by incorporating S-SiO_2	1209 mW m^{-2} vs. 290 mW m^{-2} with Nafion 117	Oxygen mass transfer coefficient decreased with the increase in S-SiO_2 into the SSBES matrix, up to 0.67×10^{-5} cm s^{-1}	[163]
AEM			
QPEEK	60 W m^{-3} vs. 52 W m^{-3} with the commercial AMI-7001 from Membrane International Inc., NJ	O_2 mass transfer coefficient and diffusion coefficient were 2.1×10^{-4} cm s^{-1} and 4.8×10^{-8} cm^2 s^{-1} for QPEEK, and 1.6×10^{-4} cm s^{-1} and 3.1×10^{-7} cm^2 s^{-1} for AMI 7001	[141]
Organic-inorganic hybrid AEM composed of QAPVA and TiO_2	125.4 mW m^{-2} vs. 65 mW m^{-2} with Nafion 117 (here comparison was made with an CEM)	Lower O_2 mass transfer coefficient of 0.05×10^{-4} vs. 0.3×10^{-4} cm s^{-1} with Nafion 117	[137]
QPEI	612 mW m^{-2} vs. 565 mW m^{-2} with AMI-7001	O_2 mass transfer coefficient and diffusion coefficient were 2.3×10^{-5} cm s^{-1} and 4.7×10^{-7} cm^2 s^{-1} for QPEI, and 0.1×10^{-5} cm s^{-1} and 3×10^{-7} cm^2 s^{-1} for AMI 7001	[142]
QPSU membrane modified with FGO	1036 mW m^{-2} vs. 576 mW m^{-2} with AMI 7001		[164]

FGO: functionalized graphene oxide.
GO-PVA-STA: graphene oxide, poly(vinyl alcohol) and silicotungstic acid.
PVA: poly(vinyl alcohol).
QAPVA: quaternized poly(vinyl alcohol).
QPEEK: quaternized poly(ether ether ketone).
QPEI: quaternized poly(ether imide).
QPSU: quaternized polysulfone.
SPEEK: sulfonated poly(ether ether ketone).
SSEBS: sulfonated polystyrene ethylene butylene polystyrene.

The energy cost of a BPM is too high if energy production is the main objective envisaged and, in our opinion, BPM should be reserved for specific objectives, in which pH balance is crucial. Some clever associations of BPM with MFCs have been proposed to produce alkali and ensure desalination [173] or to remove organic and zinc contamination in parallel effluent streams [174].

5.4. Reverse and forward osmosis (RO/FO) membrane

5.4.1. Characteristics and theoretical advantages and limit

RO membranes are used in large scale industrial units for desalination and water treatment [129,175,176]. In RO units, membranes are operated by achieving a hydrostatic pressure greater than the osmotic pressure so as to drive water transfer through the membrane against the natural direction of osmosis, while the salts are retained and concentrated on the influent surface of the membrane. Forward osmosis has also been envisioned to produce electrical power from a salinity gradient [177,178]. In this case, water transfer from a low-concentration solution (e.g. a river) to a high-concentration solution (e.g. the sea) increases the pressure of the high-concentration side, which is utilized to drive a turbine.

RO and FO membranes are similar from the point of view chemistry and separation characteristics. RO membranes, which generally have to support higher pressure than FO membranes, may be designed with a stronger mechanical resistance. RO/FO membranes are composed of polymer material that forms a layered, web-like structure [175,179]. They do not have distinguishable pores and are considered to be essentially non-porous. Theoretically, all dissolved and suspended material is rejected, even the smallest

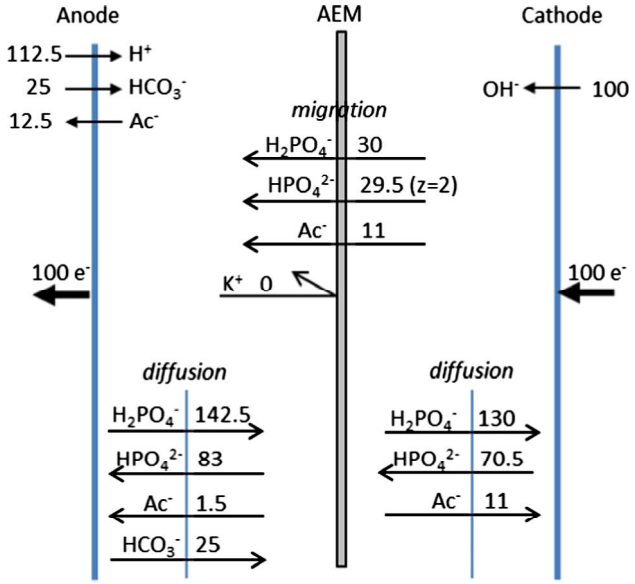

Fig. 5. Balance sheet of the molecular fluxes with an anion exchange membrane (AEM). The electrolyte is composed of 50 mM phosphate buffer and 10 mM potassium acetate.

contaminants such as monovalent ions, and water is considered to be the only material passing through the membrane [129,180]. Practically, RO membranes have salt rejection of more than 90%.

FO membranes have been implemented in MFCs to provide a water flux from the anode to the cathode compartment [101]. The anode compartment has the common salt content appropriate for microbial growth, while the salt concentration is considerably higher in the cathode compartment. Due to the salt gradient, osmosis drives water molecules from the anode to the cathode. Theoretically, all ions are rejected by the membrane, except protons, which are driven through it by the water flux because of their very small size. In this case, in theory, the transport number of proton is 1, while any other ion has a transport number of zero (Fig. 6).

In the context of MFCs, this situation is an exceptional case, in which protons are responsible for all current carried through the separator. Consequently, in theory, using an osmosis membrane is an ideal solution to achieve perfect pH balance in the MFC. Unfortunately, in return, the MFC performance is severely limited because current transport in solution is ensured only by protons, the concentration of which is generally below 10^{-6} M (pH 6) to prevent the bioanode from becoming deactivated. Proton concentration at pH around neutrality is too low to ensure high current density. Moreover, the possible benefit of adding a supporting salt to carry the current is also lost with such membranes. In the present state of the art of bioanode development, osmosis MFCs are not an effective solution when the aim is to considerably enhance power production. As mentioned in Section 5.1.1, in this context too, designing efficient acidophilic microbial anodes would be a crucial challenge.

5.4.2. Experimental work

Experimental studies have confirmed that osmosis membranes perform better than AEM or CEM because of proton transfer to the cathode side (Table 7). Moreover, it has been observed that the water flux and the high membrane resistance prevent oxygen diffusion to the anode [101]. The high salt concentration in the cathode compartment is another advantage as it significantly decreases the MFC internal resistance. Qin et al. observed that increasing NaCl concentration from 1 to 35 g L^{-1} decreased the osmosis membrane resistance from 17.6 to 5.3 Ω, while a CEM resistance decreased from 22.6 to only 9.6 Ω [181].

In conventional RO processes, several fouling mechanisms have been reported. A large variety of contaminants exist, including suspended particulate matter [inorganic or organic] and biogenic materials [129,175,176,179]. Suspended and colloidal particles coagulate together and adsorb, forming a cake-like layer on the membrane surface, while dissolved organics can interact directly with the membrane surface [184,185]. In MFCs also, osmosis membranes have been shown to be sensitive to biofouling on the bioanode side and fouling on both sides [182,186]. In conventional RO bioreactors, biofouling is mitigated by intermittent vigorous air bubbling; this solution might be adapted to MFC by bubbling nitrogen to respect anaerobiosis.

6. Porous separators

6.1. Classification and basics

Porous separators reject molecules according to their size and shape, and charge in the specific case of nanofiltration membranes. Nanofiltration (NF), ultrafiltration (UF) and microfiltration (MF) membranes retain small particles (e.g. ions, aqueous salts, viruses) in order of increasing size. The term macroporous separators, less accurately defined, aggregates various kinds of separators that retain only particles of large size such as bacteria, sands or colloids. Porous separators are less expensive than ion-exchange membranes and some common macroporous materials can even reach very low cost. Macrofiltration and UF membranes are the most commonly studied in the MFC field, whereas no or very few data are available concerning NF membranes (Table 8). As for non-porous membranes, experimental data about oxygen diffusion can differ significantly from one study to the other.

In theory, with the exception of nanofiltration membranes (see Section 6.1), porous separators do not exert selectivity in ion transfer. The balance sheets are consequently identical to that found in the absence of a separator (Fig. 2) but the mass transfer rates are reduced. Non-porous separators form a barrier to mass transfers with a strength that decreases from NF membranes to macroporous materials. According to the functions identified in Section 4.1,

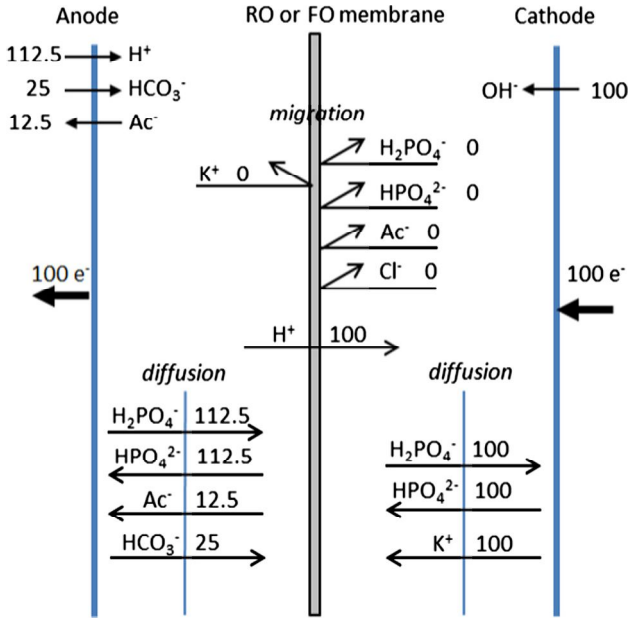

Fig. 6. Balance sheet of the molecular fluxes with a reverse/forward osmosis membrane (RO/FO). The electrolyte is composed of 50 mM phosphate buffer and 10 mM potassium acetate. Addition of KCl does not modify the theoretical balance sheet.

Table 7
Performance of osmosis membrane vs. CEM, AEM and FO membrane.

Nature	MFC performance	Comment	Ref.
Hydration Technology Innovations, LLC, Albany, OR	43 W m^{-3} vs. 40 and 23 W m^{-3} with AEM and CEM respectively	Lower pH of the catholyte with the osmosis membrane	[182]
Hydration Technology Innovations, Albany, USA	4.7 W m^{-3} vs. 3.5 W m^{-3} with CEM (Membrane International Inc., Ringwood, NJ)		[101]
Hydration Technology Innovations, LLC, Albany, OR, USA	12.57 W m^{-3} vs. 9.4 and 10.71 W m^{-3} for CEM (Nafion 117) and AEM (AMI-7001, Membrane Inc., USA) respectively	Higher anolyte conductivity with osmosis membrane	[102]
Hydration Technology Innovations, LLC, Albany, OR	75.2 A m^{-3} vs. 42.8 A m^{-3} for a MFC with CEM (not mentioned)	Higher conductivity of the osmosis membrane due to the high salinity of the cathode compartment	[181]
Hydration Technology Innovations, LLC, USA modified with silver nanoparticles (nAg) deposited on a polydopamine (pDA) coated membrane surface	61.5 mW m^{-2} vs. 55.2 mW m^{-2} for a MFC with the pristine FO membrane	Lower internal resistance of the nAg-pDA coated FO membrane in consequence of significant changes in membrane characteristics	[183]

it can be predicted that oxygen transfer to the bioanode and fuel or cation transfer to the cathode (items 1, 2 and 4 in Section 4.1) are thwarted with an efficiency that decreases from NF membranes to macroporous separators. In return, the ease with which ions cross the separator increases from NF membranes to macroporous materials (item 3), so that buffer balance is more easily achieved in this order.

6.2. Nanofiltration (NF) membrane

With pore diameters between 10 and 100 Å, NF membranes retain small particles of about the size of water molecules, sugars or aqueous salts. They fall into a transition region between RO and UF membranes. Typically, RO and UF membranes have salt rejection of more than 90% and less than 5% respectively, while NF membranes reject between 20 and 80% [189]. They are categorized by their molecular weight cut-off (MWCO expressed in Daltons (Da)), a loosely defined term that generally means the molecular weight of the globular protein molecule that is 95% rejected by the membrane [190]. MWCO is accepted to range from around 250 to 2000 Da for NF membranes [129].

Retention mechanisms involved in NF membranes are based on both the size and the charge of molecules. Ions are retained by interactions of the ion charge with the membrane, whereas water is transported through the membrane. Multivalent ions have higher rejection than monovalent ions because charge interactions are stronger [191]. NF membranes are generally negatively charged and applications consequently often deal with the elimination of anions, such as removal of sulfate [192], nitrate [193,194] or arsenic from drinking water present in the form of arsenate AsO_4^{3-} [195]. Nevertheless, removal of cations, e.g. cobalt from nuclear liquid waste [196] has also been proposed. NF membranes are known to suffer from fouling especially during wastewater reclamation [179].

To our knowledge, NF membranes have never been tested in MFCs so far. From their very small pore size, it may be predicted that they could efficiently reduce oxygen and fuel crossover. In return, it can be feared that they would create high resistance to ion transfer but probably less than ion-selective membranes, which are widely used in MFCs. In consequence, NF membranes may be interesting candidates deserving to be tested as MFC separators.

6.3. Ultrafiltration (UF) membrane

UF membranes, with pore diameters in the 100–1000 Å range, are mostly used to separate small colloidal particles [190]. Their MWCO varies between 2000 and 500,000 Da [34,129]. Yang and He dedicated a large part of their recent review on integrating UF membranes in bioelectrochemical systems [34].

UF membranes have not been widely investigated in MFCs. Kim et al. compared various UF membranes (DIAFLO ultrafiltration, Amicon, Inc., MA) with a CEM and an AEM (CMI-7000 and AMI-7001, both from Membrane International Inc., NJ) as MFC separators [133]. The results depended strongly on membrane MWCO. The MFC internal resistance was significantly higher (6009 Ω) with the 0.5 kDa UF membrane than with the others (1239 and 1233 Ω for 1 and 3 kDa respectively). The same trend was confirmed when the anode-cathode distance was reduced from 12 to 4 cm (1814 Ω versus 98 Ω and 91 Ω, respectively). Oxygen mass transfer coefficients of the UF-membranes were smaller than those measured for the other membranes, including Nafion 117, CEM and AEM. The smallest coefficient was achieved by the 0.5 kDa UF membrane (0.19×10^{-4} cm s^{-1}), which also showed the lowest acetate mass transfer coefficient (0.89×10^{-8} cm s^{-1}). In contrast, the 1 kDa and 3 kDa UF membranes were the most permeable to acetate (16×10^{-8} cm s^{-1} and 27×10^{-8} cm s^{-1} respectively). This study presents UF membranes with low MWCO as valid MFC separator candidates.

Nevertheless, the MFCs equipped with Nafion 117 or with the UF membranes delivered similar power densities, ranging from 36 to 38 mW m^{-2}. The authors concluded that the high internal resistance due to the 12-cm inter-electrode distance was the limiting step, which precluded comparison of membrane impact. This study nicely illustrates the necessity to accurately characterize the experimental device used to compare membrane performance. Similar results have been reported by comparing a 1 kDa UF membrane (DIAFLO ultrafiltration, Amicon Inc., USA) with a Nafion membrane, which led to similar power densities of 53.5 mW m^{-2} and 55.7 mW m^{-2}, respectively [197]. In contrast, Hou et al., testing UF membranes with different MWCO (1, 5 and 10 kDa) in a single-compartment MFC, observed the highest maximum power density with the 1 kDa membrane (324 mW m^{-2}) [198]. It should be emphasized here that comparison of membrane performance achieved in MFCs should be taken with great caution. MFCs may be controlled by several limiting steps, including the solution ohmic drop, the bioanode kinetics or the cathode kinetics, or combinations of several of these steps. Comparing membrane performance in an MFC requires the MFC be designed so that the membrane is the rate-limiting step.

Attempts have been made to reduce the membrane resistance by enhancing its hydrophilic character. With this aim, the surface of a UF membrane was coated with polydopamine (PD), which has similar capability to a mussel's adhesive foot protein [199]. MFC power generation was improved by 15% due to an enhanced hydrophilicity on the UF membrane that caused a greater retention of electrolytes at the solution-membrane interface. Furthermore, PD coating on UF membranes can delay biofouling by hindering the attachment of EPSs and bacterial cells, which block the membrane pores.

Table 8
Characteristics of porous separators reported in the MFC literature. Both manufacturer's data and parameters calculated from experimental data are given. Manufacturer's data are indicated by an asterisk ∗.

Membrane	Thickness (mm)	Pore diameter (mm)	Porosity (%)	Internal resistance (Ω)	Oxygen mass transfer ko ($cm\ s^{-1}$)	Oxygen diffusion coefficient Do ($cm^2\ s^{-1}$)	Acetate mass transfer ka ($cm\ s^{-1}$)	Acetate diffusion coefficient Da ($cm^2\ s^{-1}$)	Ref.
Ultrafiltration									
UF-0.5K	265*			6009	0.19×10^{-4}	0.51×10^{-6}	0.89×10^{-8}	0.24×10^{-9}	[133]
UF-1K	265*			1239	0.41×10^{-4}	1.1×10^{-6}	16×10^{-8}	4.2×10^{-9}	
UF-3K	265*			1233	0.42×10^{-4}	1.1×10^{-6}	27×10^{-8}	7.2×10^{-9}	
(DIAFLO ultrafiltration. Amicon. Inc., MA)									
M-10 (Montmorillonite 10%)				118	2.96×10^{-5}	8.1×10^{-6}	3.23×10^{-5}	8.06×10^{-6}	[187]
M-15				96	1.94×10^{-5}	9.71×10^{-6}	2.60×10^{-5}	6.51×10^{-6}	
M-20				78	1.09×10^{-5}	4.35×10^{-6}	2.38×10^{-5}	5.96×10^{-6}	
K-20 (Kaolinite 20%)				104	2.05×10^{-5}	8.13×10^{-6}	2.93×10^{-5}	7.31×10^{-6}	
Microfiltration									
Q/IEF J01 Shanghai Xingya Co., Shanghai	130	0.45		263	5.9×10^{-4}	7.7×10^{-6}			[188]
Supor. Pall Co.. MI. USA	132*	0.1*			1.13×10^{-3}	1.49×10^{-5}			[70]
(Hydrophilic polyethersulfone	145*	0.2*			1.27×10^{-3}	1.84×10^{-5}			
PES)	140*	0.45*			2.27×10^{-3}	3.17×10^{-5}			
Durapore (polyvinylidene fluoride PVDF)	125*	0.1*	70		3.27×10^{-3}	4.08×10^{-5}			[70]
		0.22*			1.87×10^{-3}	2.33×10^{-5}			
		0.45*			11×10^{-3}	13.8×10^{-5}			
Macrofiltration									
Glass fiber 1.0	400			2.26	5×10^{-5}	5×10^{-6}			[100]
Glass fiber 0.4	1000			2.39	7.5×10^{-5}	3×10^{-6}			
J-cloth	300			0.21	290×10^{-5}	86.9×10^{-6}			[100]
PP80 (nonwoven fabric)				480	30×10^{-4}	3×10^{-6}			[138]
PP100 (nonwoven fabric)				535	20×10^{-4}	9×10^{-6}			
PPS (textile fabric)				779	50×10^{-4}	2.6×10^{-6}			
S-PPS (sulfonated polyphenylene sulfide)				519	34×10^{-4}	18×10^{-6}			
Cellulose (cellulose-ester)				481	11×10^{-4}	1.5×10^{-6}			
PP80 (nonwoven fabric)	490	30		9.29	3.7×10^{-5}	1.8×10^{-6}			[139]
PP100 (nonwoven fabric)	540	42		9.5	7.3×10^{-5}	3.7×10^{-6}			
PPS (textile fabric)	520	40		9.51	7.5×10^{-5}	3.9×10^{-6}			
S-PPS (sulfonated polyphenylene sulfide)	540	44		3.53	7.2×10^{-5}	3.7×10^{-6}			

Ceramic separators have also been reported in the recent MFC literature [33,185,200]. They are considered to be porous separators and can be classified as UF or MF membranes. Ghadge and Ghangrekar developed a ceramic separator made from red soil blended with cation exchanger, montmorillonite and kaolinite [187]. Addition of 20% montmorillonite in clay yielded better conductivity of the separator and hence higher energy recovery. Winfield et al., testing two types of ceramic, showed that earthenware provided better performances than terracotta ($2.83\ W\ m^{-3}$ vs. $3.66\ W\ m^{-3}$) [201] with quite a long operation time of 6 weeks. In another study, earthenware was compared to a CEM. The earthenware-MFC provided current for 8 months and generated power densities comparable to those of the CEM-MFC, up to $4.5\ W\ m^{-3}$ [200].

6.4. Microfiltration (MF) membrane

MF membranes, with pore diameters ranging from 1000 to 10^4 Å, reject particles such as solids, colloidal particles and bacteria, while even proteins pass through [180]. MF membranes are commonly used for wastewater treatment and a few studies have tested them for MFCs.

Biffinger et al. tested polymer filters made of regenerated cellulose (Fisherbrand, 12,000–14,000 Da, 20 μm wall thickness), cellulose nitrate (Millipore, 0.2 μm pore size, 125 μm thickness), nylon (Whatman, 0.2 μm pore size, 20 μm thickness) and polycarbonate (Millipore, GTTP, 0.2 μm pore size, 20 μm thickness), which were considered as nanoporous, although these materials are principally used to create MF membranes [202]. These separators were

compared to Nafion 117 in a miniature MFC. MFCs produced comparable power densities ranging from 16 W m^{-3} to 6 W m^{-3} for cellulose nitrate, of the same order of magnitude as those obtained with Nafion (11 W m^{-3}). They also exhibited comparable durability, up to 500 h, to Nafion-117 membranes. Interestingly, no pH gradient between the two compartments was observed with the polycarbonate membrane.

Cellulose acetate MF membrane (Q/IEF J01 Shanghai Xingya Co., Shanghai) have been compared with Nafion 117 in a two-compartment MFC [188]. As predicted, CE was smaller with the MF membrane (38.5 vs. 74.7% with Nafion 117) due to the higher oxygen mass transfer coefficient (5.9×10^{-4} vs. 1.4×10^{-4} cm s^{-1} for MF and Nafion 117, respectively). Lower CE can also be explained by fuel diffusion to the cathode compartment. The pH gradient was reduced: pH values were 6.9 and 8 in the anode and cathode compartments respectively with the MF membrane, vs. 6.4 and 9.5 with Nafion 117. Nevertheless, similar power densities were obtained (0.831 W m^{-2} and 0.872 W m^{-2}, respectively). It was concluded that MF membranes could parallel PEM in power density while decreasing the separator cost [153]. Here again, the equality of the power produced may also indicate that the membrane was not a rate-limiting step in the MFC. For instance, MF membranes compared to a PEM in an air cathode, single-compartment MFC have led to different conclusions [203]. The lower internal resistance obtained with the MF membrane (248 Ω vs. 672 Ω with PEM) resulted in higher power: 214 mW m^{-2} with the MF membrane against 103 mW m^{-2} with PEM. Once again, the cell configuration may have had a major impact on the conclusions that could be drawn about membrane suitability.

Recently, MF membranes (hydrophilic polyethersulfone PES, Supor® from Pall Co., MI, USA, and poly(-vinylidene fluoride) PVDF, Durapore® from Millipore Co., MA, USA) have been tested in an air-cathode single-compartment MFC, paying particular attention to the fouling mechanisms of the air-cathode [70]. Oxygen mass transfer coefficients of the MF membranes were confirmed to be higher than that of Nafion 117 (Table 8).

6.5. Macrofiltration

Macroporous separators reject only species of very large size, such as bacteria and yeasts, or even retain only macro-particles such as granules. They have been widely tested in MFCs, especially because of their low cost and easy availability. From a theoretical point of view, their macro-porosity should benefit the pH balance between the anode and cathode compartments but should be detrimental to oxygen and substrate crossover.

The range of macroporous materials that can be used is limited only by the imagination of researchers. Technologically advanced material such as Zirfon has been tested in a two-compartment MFC [153]. Zirfon is a macroporous organomineral material containing 85 wt% of hydrophilic ZrO_2 powder and 15 wt% polysulfone. The lower resistance than with Nafion was confirmed experimentally (2727 Ω cm vs. 17,000 Ω cm) but so was a higher permeability to oxygen (1.9×10^{-3} cm s^{-1} vs. 2.8×10^{-4} cm s^{-1}, respectively), which globally led to lower MFC performances than Nafion.

On the other hand, material as simple and cheap as J-Cloth has also been investigated several times [100,126,204]. The oxygen flux through this material is high (290×10^{-5} cm s^{-1}) but the main advantage lies in its capability to support the development of an intermediate biofilm, which has been observed as a factor that increases power, by consuming oxygen before it can reach the anode. This aerobic biofilm may be thought of as a preliminary proof of the concept of the "Microbial separator" proposed in Section 3.2 Glass fiber has also demonstrated good capacities as a porous separator [100,204] [205,206]. It led to higher CE than J-Cloth, probably due to its lower oxygen mass transfer coefficient (5.0×10^{-5} cm s^{-1}) [100].

In the long term, J-Cloth is handicapped by its biodegradability. Nevertheless, the biodegradability of the separator is not always a disadvantage. An MFC equipped with latex rubber as separator started to produce current after 3 weeks and then showed continuous improvement over time. After 6 months, it reached higher power and current than a similar MFC equipped with an AEM. After 11 months, performance declined with both AEM and PEM but continued to increase with the latex separator [207]. Biodegradation of the material resulted in pores forming through the separator, which improved the MFC performance. Building on this success, the same group has recently investigated a biodegradable bag as a macroporous membrane separator [208]. The MFC began to produce power after 2 weeks and displayed continuous improvement. After 7 months, the performance decreased and damage was visible, so the bag material was no longer able to provide sufficient separation. From a general point of view, biodegradability of whole MFC is starting to be viewed as an important advantage.

Different nonwoven polypropylene, polyphenylene sulfide and cellulose-ester fabrics also led to comparable or slightly better MFC performance than Nafion 117 and CEM (CMI-7000, Memb. Inc., USA) because of their smaller ohmic resistance [138]. The higher oxygen mass transfer compared to Nafion and CEM led to lower CEs. Another study comparing textile fabrics of polyphenylene sulfide, sulfonated polyphenylene sulfide and the nonwoven fabrics of polypropylene to Nafion 117 and CEM (CMI-7000) revealed a greater difference in terms of power density produced (up to 190 mW m^{-2} with macroporous separators vs. 24 mW m^{-2} with Nafion 117) and surprisingly similar or lower oxygen mass transfer coefficients than that of Nafion (Table 8) [139].

7. Concluding remarks

In the current state of the art, most MFCs use low conductivity electrolytes at around neutral pH. This situation may change if efficient halotolerant, acidophilic or alkaliphilic microbial anodes were designed, but these objectives remain research challenges. Work in these directions should be encouraged. Because of the nutriments, salts and trace elements required for microbial growth, MFCs seem condemned to work with chemically complex electrolytes, which may raise various causes of electrode deactivation. Local acidification of the bioanode and local alkalinization of the cathode are also important pathways to electrode deactivation. In this context, ion transport through the electrolyte is the central crossroad, which controls the MFC performance and long-term behaviour.

This review gives an easy-to-use theoretical tool to predict the behaviour of an MFC on the basis of the ionic contents of the electrolyte. The theory should motivate the redirection of certain research routes on MFC separators and boost some others. For instance, it is shown that, except in osmotic MFCs, proton transport has no role in current carrying in the pH range of the electrolytes used so far. This has already been claimed by a several research groups but too many studies still focus on proton transport and try to improve PEM to enhance MFC power production.

The awkward problem of pH balance inside the cell is another essential issue in MFC development. Proton migration from the anode to the cathode has no significant impact and migration of the buffering anionic species helps to mitigate the bioanode acidification only moderately. This situation is very different from that in chemical hydrogen fuel cells, which have often been used as model to understand MFC mechanisms. Controlling the pH gradient is a crucial requirement, though a tricky task, to optimize

MFC performance. The theoretical framework presented here should now allow dedicated theoretical approaches, e.g. to optimize buffer composition, including multispecies buffers.

Separator-less MFCs could be of considerable interest as far as loss of a part of the fuel may be accepted as the price to be paid for a device that is simple to implement. This constraint should be perfectly acceptable in the context of waste treatment for example. In this context, the concept of "microbial separator" may be a promising way to control fuel and oxygen transport inside the MFC.

Using a suitable separator may be an effective way to drive ion transport towards a specific pattern but it may also be detrimental. The advantages/disadvantages of the various kinds of membranes and separators are compared in the light of theory and the conclusions are confronted with the experimental data reported in the literature. In the context of ion-exchange membranes, AEMs would possibly be better candidate MFC separators than CEM if the objective is to increase power at the price of lower Coulombic efficiency. Nevertheless, in our opinion, ion exchange membranes should mainly be implemented when the MFC has a target other than power generation, such as desalination, separation, and sensing. If the only goal is power supply, porous separators, less costly, propose a continuum of transfer characteristics that should be appropriate for most MFCs.

Concerning the essential issue of oxygen transfer, large discrepancies are observed among the experimental data; this item deserves deeper and dedicated investigations. The analysis of many experimental studies points out the need to perfectly characterize the experimental set-up in order to draw sound conclusions on membrane suitability. The fact that different membranes lead an MFC to provide similar power does not always prove the equivalence of the membranes tested; it may also indicate that a step other than ion transfer through the membrane is rate-limiting. Specific experimental devices should now be designed for comparing membranes in MFCs, ensuring that ion transfer through the membrane is the rate-limiting step. Conventional studies performed in the domain of membrane processes should be a suitable source of inspiration.

Acknowledgements

This work benefited from the support of the French state, managed by the Agence Nationale de la Recherche (ANR), within the framework of the project Bioelec (ANR-13-BIME-006).

References

[1] Kim BH, Ikeda T, Park HS, Kim HJ, Hyun MS, Kano K, et al. Electrochemical activity of an Fe(III)-reducing bacterium, *Shewanella putrefaciens* IR-1, in the presence of alternative electron acceptors. Biotechnol Tech 1999;13(7):475–8.
[2] Bond DR, Holmes DE, Tender LM, Lovley DR. Electrode-reducing microorganisms that harvest energy from marine sediments. Science 2002;295(5554):483–5.
[3] Tender LM, Reimers CE, Stecher HA, Holmes DE, Bond DR, Lowy DA, et al. Harnessing microbially generated power on the seafloor. Nat Biotechnol 2002;20(8):821–5.
[4] Reimers CE, Tender LM, Fertig S, Wang W. Harvesting energy from the marine sediment-water interface. Environ Sci Technol 2001;35(1):192–5.
[5] Bergel A, Feron D, Mollica A. Catalysis of oxygen reduction in PEM fuel cell by seawater biofilm. Electrochem Commun 2005;7(9):900–4.
[6] Pant D, Van Bogaert G, Diels L, Vanbroekhoven K. A review of the substrates used in microbial fuel cells (MFCs) for sustainable energy production. Bioresour Technol 2010;101(6):1533–43.
[7] Pandey P, Shinde VN, Deopurkar RL, Kale SP, Patil SA, Pant D. Recent advances in the use of different substrates in microbial fuel cells toward wastewater treatment and simultaneous energy recovery. Appl Energy 2016;15(168):706–23.
[8] Lovley DR, Nevin KP. A shift in the current: new applications and concepts for microbe-electrode electron exchange. Curr Opin Biotechnol 2011;22(3):441–8.
[9] Tremblay P-L, Zhang T. Electrifying microbes for the production of chemicals. Front Microbiol 2015;11(6):UNSP 201.
[10] Schroeder U, Harnisch F, Angenent LT. Microbial electrochemistry and technology: terminology and classification. Energy Environ Sci 2015;8(2):513–9.
[11] Sleutels THJA, Ter Heijne A, Buisman CJN, Hamelers HVM. Bioelectrochemical systems: an outlook for practical applications. Chemsuschem 2012;5(6):1012–9.
[12] Wang H, Luo H, Fallgren PH, Jin S, Ren ZJ. Bioelectrochemical system platform for sustainable environmental remediation and energy generation. Biotechnol Adv 2015;33(3–4):317–34.
[13] Wang H, Ren ZJ. A comprehensive review of microbial electrochemical systems as a platform technology. Biotechnol Adv 2013;31(8):1796–807.
[14] Logan BE, Rabaey K. Conversion of wastes into bioelectricity and chemicals by using microbial electrochemical technologies. Science 2012;337(6095):686–90.
[15] Li W-W, Yu H-Q, He Z. Towards sustainable wastewater treatment by using microbial fuel cells-centered technologies. Energy Environ Sci 2014;7(3):911–24.
[16] Zhang Y, Angelidaki I. Microbial electrolysis cells turning to be versatile technology: recent advances and future challenges. Water Res 2014;1(56):11–25.
[17] Escapa A, Mateos R, Martinez EJ, Blanes J. Microbial electrolysis cells: an emerging technology for wastewater treatment and energy recovery. From laboratory to pilot plant and beyond. Renew Sustain Energy Rev 2016;55:942–56.
[18] Lovley DR, Nevin KP. Electrobiocommodities: powering microbial production of fuels and commodity chemicals from carbon dioxide with electricity. Curr Opin Biotechnol 2013;24(3):385–90.
[19] Harnisch F, Schroeder U. From MFC to MXC: chemical and biological cathodes and their potential for microbial bioelectrochemical systems. Chem Soc Rev 2010;39(11):4433–48.
[20] Davis JB, Yarbrough HFJ. Preliminary experiments on a microbial fuel cell. Science 1962;137(3530):615–6.
[21] Erable B, Feron D, Bergel A. Microbial catalysis of the oxygen reduction reaction for microbial fuel cells: a review. Chemsuschem 2012;5(6):975–87.
[22] Rimboud M, Pocaznoi D, Erable B, Bergel A. Electroanalysis of microbial anodes for bioelectrochemical systems: basics, progress and perspectives. Phys Chem Chem Phys 2014;16(31):16349–66.
[23] Logan BE. Exoelectrogenic bacteria that power microbial fuel cells. Nat Rev Microbiol 2009;7(5):375–81.
[24] Schaetzle O, Barriere F, Baronian K. Bacteria and yeasts as catalysts in microbial fuel cells: electron transfer from micro-organisms to electrodes for green electricity. Energy Environ Sci 2008;1(6):607–20.
[25] Rousseau R, Dominguez-Benetton X, Delia M-L, Bergel A. Microbial bioanodes with high salinity tolerance for microbial fuel cells and microbial electrolysis cells. Electrochem Commun 2013;33:1–4.
[26] Karthikeyan R, Selvam A, Cheng KY, Wong JW-C. Influence of ionic conductivity in bioelectricity production from saline domestic sewage sludge in microbial fuel cells. Bioresour Technol 2016;200:845–52.
[27] Martinucci E, Pizza F, Perrino D, Colombo A, Trasatti SPM, Barnabei AL, et al. Energy balance and microbial fuel cells experimentation at wastewater treatment plant Milano-Nosedo. Int J Hydrogen Energy 2015;40(42):14683–9.
[28] Jannelli N, Nastro RA, Cigolotti V, Minutillo M, Falucci G. Low pH, high salinity: too much for microbial fuel cells? Appl Energy 2016 [available online 3 August 2016].
[29] Dhar BR, Lee H-S. Membranes for bioelectrochemical systems: challenges and research advances. Environ Technol 2013;34(13–14):1751–64.
[30] Daud SM, Kim BH, Ghasemi M, Daud WRW. Separators used in microbial electrochemical technologies: current status and future prospects. Bioresour Technol 2015;195:170–9.
[31] Li W-W, Sheng G-P, Liu X-W, Yu H-Q. Recent advances in the separators for microbial fuel cells. Bioresour Technol 2011;102(1):244–52.
[32] Leong JX, Daud WRW, Ghasemi M, Ben Liew K, Ismail M. Ion exchange membranes as separators in microbial fuel cells for bioenergy conversion: a comprehensive review. Renew Sustain Energy Rev 2013;28:575–87.
[33] Winfield J, Gajda I, Greenman J, Ieropoulos I. A review into the use of ceramics in microbial fuel cells. Bioresour Technol 2016;215:296–303.
[34] Yuan H, He Z. Integrating membrane filtration into bioelectrochemical systems as next generation energy-efficient wastewater treatment technologies for water reclamation: a review. Bioresour Technol 2015;195:202–9.
[35] Sevda S, Yuan H, He Z, Abu-Reesh IM. Microbial desalination cells as a versatile technology: functions, optimization and prospective. Desalination 2015;1(371):9–17.
[36] Xu L, Zhao Y, Doherty L, Hu Y, Hao X. The integrated processes for wastewater treatment based on the principle of microbial fuel cells: a review. Crit Rev Environ Sci Technol 2016;46(1):60–91.
[37] Varcoe JR, Atanassov P, Dekel DR, Herring AM, Hickner MA, Kohl PA, et al. Anion-exchange membranes in electrochemical energy systems. Energy Environ Sci 2014;7(10):3135–91.
[38] Harnisch F, Warmbier R, Schneider R, Schroeder U. Modeling the ion transfer and polarization of ion exchange membranes in bioelectrochemical systems. Bioelectrochemistry 2009;75(2):136–41.

[39] Popat SC, Ki D, Young MN, Rittmann BE, Torres CI. Buffer pK(a) and transport govern the concentration overpotential in electrochemical oxygen reduction at neutral pH. Chemelectrochem 2014;1(11):1909–15.
[40] Harnisch F, Schroeder U. Selectivity versus Mobility: Separation of Anode and Cathode in Microbial Bioelectrochemical Systems. Chemsuschem 2009;2 (10):921–6.
[41] Popat SC, Torres CI. Critical transport rates that limit the performance of microbial electrochemistry technologies. Bioresour Technol 2016;215:265–73.
[42] Rousseau R, Santaella C, Achouak W, Godon J-J, Bonnafous A, Bergel A, et al. The electrochemical kinetics of high-salinity tolerant bioanodes is correlated with the structure and microbial composition of the biofilm. ChemElectroChem 2014;1:1–11.
[43] Tender LM, Gray SA, Groveman E, Lowy DA, Kauffman P, Melhado J, et al. The first demonstration of a microbial fuel cell as a viable power supply: powering a meteorological buoy. J Power Sources 2008;179(2):571–5.
[44] An J, Nam J, Kim B, Lee H-S, Kim BH, Chang IS. Performance variation according to anode-embedded orientation in a sediment microbial fuel cell employing a chessboard-like hundred-piece anode. Bioresour Technol 2015;190:175–81.
[45] Christgen B, Scott K, Dolfing J, Head IM, Curtis TP. An evaluation of the performance and economics of membranes and separators in single chamber microbial fuel cells treating domestic wastewater. PLoS ONE 2015;10(8): e0136108.
[46] Heidrich ES, Edwards SR, Dolfing J, Cotterill SE, Curtis TP. Performance of a pilot scale microbial electrolysis cell fed on domestic wastewater at ambient temperatures for a 12 month period. Bioresour Technol 2014;173:87–95.
[47] Dopson M, Ni G, Sleutels THJA. Possibilities for extremophilic microorganisms in microbial electrochemical systems. FEMS Microbiol Rev 2016;40 (2):164–81.
[48] Pocaznoi D, Erable B, Etcheverry L, Delia M-L, Bergel A. Towards an engineering-oriented strategy for building microbial anodes for microbial fuel cells. Phys Chem Chem Phys 2012;14(38):13332–43.
[49] Blanchet E, Pécastaings S, Erable B, Roques C, Bergel A. Protons accumulation during anodic phase turned to advantage for oxygen reduction during cathodic phase in reversible bioelectrodes. Bioresour Technol 2014;173:224–30.
[50] Ketep SF, Bergel A, Bertrand M, Achouak W, Fourest E. Lowering the applied potential during successive scratching/re-inoculation improves the performance of microbial anodes for microbial fuel cells. Bioresour Technol 2013;127:448–55.
[51] Zhang E, Zhai W, Luo Y, Scott K, Wang X, Diao G. Acclimatization of microbial consortia to alkaline conditions and enhanced electricity generation. Bioresour Technol 2016;211:736–42.
[52] Gil GC, Chang IS, Kim BH, Kim M, Jang JK, Park HS, et al. Operational parameters affecting the performance of a mediator-less microbial fuel cell. Biosens Bioelectron 2003;18(4):327–34.
[53] Lacroix R, Da Silva S, Gaig MV, Rousseau R, Delia M-L, Bergel A. Modelling potential/current distribution in microbial electrochemical systems shows how the optimal bioanode architecture depends on electrolyte conductivity. Phys Chem Chem Phys 2014;16(41):22892–902.
[54] Qu Y, Feng Y, Wang X, Logan BE. Use of a coculture to enable current production by *Geobacter sulfurreducens*. Appl Environ Microbiol 2012;78 (9):3484–7.
[55] Liu X-W, Li W-W, Yu H-Q. Cathodic catalysts in bioelectrochemical systems for energy recovery from wastewater. Chem Soc Rev 2014;43(22):7718–45.
[56] Ben Liew K, Daud WRW, Ghasemi M, Leong JX, Lim WS, Ismail M. Non-Pt catalyst as oxygen reduction reaction in microbial fuel cells: a review. Int J Hydrogen Energy 2014;39(10):4870–83.
[57] Wang Z, Cao C, Zheng Y, Chen S, Zhao F. Abiotic oxygen reduction reaction catalysts used in microbial fuel cells. Chemelectrochem 2014;1(11):1813–21.
[58] Noori MT, Jain SC, Ghangrekar MM, Mukherjee CK. Biofouling inhibition and enhancing performance of microbial fuel cell using silver nano-particles as fungicide and cathode catalyst. Bioresour Technol 2016 [available online 18 August 2016].
[59] Santoro C, Artyushkova K, Babanova S, Atanassov P, Ieropoulos I, Grattieri M, et al. Parameters characterization and optimization of activated carbon (AC) cathodes for microbial fuel cell application. Bioresour Technol 2014;163:54–63.
[60] Kannan MV, Kumar GG. Current status, key challenges and its solutions in the design and development of graphene based ORR catalysts for the microbial fuel cell applications. Biosens Bioelectron 2016;15(77):1208–20.
[61] Logan BE, Wallack MJ, Kim K-Y, He W, Feng Y, Saikaly PE. Assessment of microbial fuel cell configurations and power densities. Environ Sci Technol Lett 2015;2(8):206–14.
[62] Kim BH, Lim SS, Daud WRW, Gadd GM, Chang IS. The biocathode of microbial electrochemical systems and microbially-influenced corrosion. Bioresour Technol 2015;190:395–401.
[63] Schaetzle O, Barriere F, Schroeder U. An improved microbial fuel cell with laccase as the oxygen reduction catalyst. Energy Environ Sci 2009;2(1):96–9.
[64] Erable B, Etcheverry L, Bergel A. Increased power from a two-chamber microbial fuel cell with a low-pH air-cathode compartment. Electrochem Commun 2009;11(3):619–22.
[65] Popat SC, Ki D, Rittmann BE, Torres CI. Importance of OH- transport from cathodes in microbial fuel cells. Chemsuschem 2012;5(6):1071–9.
[66] Rau GH. Electrochemical splitting of calcium carbonate to increase solution alkalinity: implications for mitigation of carbon dioxide and ocean acidity. Environ Sci Technol 2008;42(23):8935–40.
[67] Tlili MM, Benamor M, Gabrielli C, Perrot H, Tribollet B. Influence of the interfacial pH on electrochemical $CaCO_3$ precipitation. J Electrochem Soc 2003;150(11):C765–71.
[68] Nair M, Misra B. Electrolytic deposition for scale control in sea-water distillation. Desalination 1978;27(1):59–64.
[69] Nair M, Misra B. Electrolytic scale formation in sea-water distillation systems. Desalination 1978;25(3):263–8.
[70] Ma J, Wang Z, Suor D, Liu S, Li J, Wu Z. Temporal variations of cathode performance in air-cathode single-chamber microbial fuel cells with different separators. J Power Sources 2014;25(272):24–33.
[71] Janicek A, Fan Y, Liu H. Performance and stability of different cathode base materials for use in microbial fuel cells. J Power Sources 2015;15 (280):159–65.
[72] Santini M, Guilizzoni M, Lorenzi M, Atanassov P, Marsili E, Fest-Santini S, et al. Three-dimensional X-ray microcomputed tomography of carbonates and biofilm on operated cathode in single chamber microbial fuel cell. Biointerphases 2015;10(3):31009.
[73] Liu H, Cheng S, Huang L, Logan BE. Scale-lip of membrane-free single-chamber microbial fuel cells. J Power Sources 2008;179(1):274–9.
[74] Harnisch F, Wirth S, Schroeder U. Effects of substrate and metabolite crossover on the cathodic oxygen reduction reaction in microbial fuel cells: platinum vs. iron(II) phthalocyanine based electrodes. Electrochem Commun 2009;11(11):2253–6.
[75] Santoro C, Babanova S, Erable B, Schuler A, Atanassov P. Bilirubin oxidase based enzymatic air-breathing cathode: operation under pristine and contaminated conditions. Bioelectrochemistry 2016;108:1–7.
[76] Liu H, Logan BE. Electricity generation using an air-cathode single chamber microbial fuel cell in the presence and absence of a proton exchange membrane. Environ Sci Technol 2004;38(14):4040–6.
[77] Liu W, Cheng S, Sun D, Huang H, Chen J, Cen K. Inhibition of microbial growth on air cathodes of single chamber microbial fuel cells by incorporating enrofloxacin into the catalyst layer. Biosens Bioelectron 2015;15(72):44–50.
[78] Yuan Y, Zhou S, Tang J. In situ investigation of cathode and local biofilm microenvironments reveals important roles of OH- and oxygen transport in microbial fuel cells. Environ Sci Technol 2013;47(9):4911–7.
[79] Tartakovsky B, Guiot SR. A comparison of air and hydrogen peroxide oxygenated microbial fuel cell reactors. Biotechnol Prog 2006;22(1):241–6.
[80] Cristiani P, Carvalho ML, Guerrini E, Daghio M, Santoro C, Li B. Cathodic and anodic biofilms in single chamber microbial fuel cells. Bioelectrochemistry 2013;92:6–13.
[81] Rismani-Yazdi H, Carver SM, Christy AD, Tuovinen IH. Cathodic limitations in microbial fuel cells: an overview. J Power Sources 2008;180(2):683–94.
[82] Scofield ME, Liu H, Wong SS. A concise guide to sustainable PEMFCs: recent advances in improving both oxygen reduction catalysts and proton exchange membranes. Chem Soc Rev 2015;44(16):5836–60.
[83] Lide DR. Handbook of chemistry and physics, internet version [Internet]. CRC Press; 2005. <http://www.hbcpnetbase.com>.
[84] Mano N, Mao F, Heller A. Characteristics of a miniature compartment-less glucose-O-2 biofuel cell and its operation in a living plant. J Am Chem Soc 2003;125(21):6588–94.
[85] Willner I, Yan Y-M, Willner B, Tel-Vered R. Integrated enzyme-based biofuel cells – a review. Fuel Cells 2009;9(1):7–24.
[86] Liu Y, Dong S. A biofuel cell harvesting energy from glucose-air and fruit juice-air. Biosens Bioelectron 2007;23(4):593–7.
[87] Cosnier S, Le Goff A, Holzinger M. Towards glucose biofuel cells implanted in human body for powering artificial organs: review. Electrochem Commun 2014;38:19–23.
[88] Barriere F, Kavanagh P, Leech D. A laccase-glucose oxidase biofuel cell prototype operating in a physiological buffer. Electrochim Acta 2006;51 (24):5187–92.
[89] Li W-W, Yu H-Q. Stimulating sediment bioremediation with benthic microbial fuel cells. Biotechnol Adv 2015;33(1):1–12.
[90] Ewing T, Ha PT, Babauta JT, Tang NT, Heo D, Beyenal H. Scale-up of sediment microbial fuel cells. J Power Sources 2014;25(272):311–9.
[91] Erable B, Lacroix R, Etcheverry L, Feron D, Delia ML, Bergel A. Marine floating microbial fuel cell involving aerobic biofilm on stainless steel cathodes. Bioresour Technol 2013;142:510–6.
[92] Jang JK, Pham TH, Chang IS, Kang KH, Moon H, Cho KS, et al. Construction and operation of a novel mediator- and membrane-less microbial fuel cell. Process Biochem 2004;39(8):1007–12.
[93] Aldrovandi A, Marsili E, Stante L, Paganin P, Tabacchioni S, Giordano A. Sustainable power production in a membrane-less and mediator-less synthetic wastewater microbial fuel cell. Bioresour Technol 2009;100 (13):3252–60.
[94] Zhuwei D, Qinghai L, Meng T, Shaohua L, Haoran L. Electricity generation using membrane-less microbial fuel cell during wastewater treatment. Chin J Chem Eng 2008;16(5):772–7.
[95] Zhan Y-L, Zhang P-P, Yan G, Wang J, Guo S. Progress in microbial fuel cell and its application. Mod Chem Ind 2007;27(1):13–7.
[96] Liu H, Cheng SA, Logan BE. Power generation in fed-batch microbial fuel cells as a function of ionic strength, temperature, and reactor configuration. Environ Sci Technol 2005;39(14):5488–93.

[97] Cheng S, Liu H, Logan BE. Increased power generation in a continuous flow MFC with advective flow through the porous anode and reduced electrode spacing. Environ Sci Technol 2006;40(7):2426–32.
[98] Guerrini E, Grattieri M, Trasatti SP, Bestetti M, Cristiani P. Performance explorations of single chamber microbial fuel cells by using various microelectrodes applied to biocathodes. Int J Hydrogen Energy 2014;39 (36):21837–46.
[99] Yang S, Jia B, Liu H. Effects of the Pt loading side and cathode-biofilm on the performance of a membrane-less and single-chamber microbial fuel cell. Bioresour Technol 2009;100(3):1197–202.
[100] Zhang X, Cheng S, Wang X, Huang X, Logan BE. Separator characteristics for increasing performance of microbial fuel cells. Environ Sci Technol 2009;43 (21):8456–61.
[101] Zhang F, Brastad KS, He Z. Integrating forward osmosis into microbial fuel cells for wastewater treatment, water extraction and bioelectricity generation. Environ Sci Technol 2011;45(15):6690–6.
[102] Zhu X-Z, Zhang F, Li W-W, Liu H-Q, Wang Y-K, Huang M-S. Forward osmosis membrane favors an improved proton flux and electricity generation in microbial fuel cells. Desalination 2015;15(372):26–31.
[103] Rozendal RA, Hamelers HVM, Buisman CJN. Effects of membrane cation transport on pH and microbial fuel cell performance. Environ Sci Technol 2006;40(17):5206–11.
[104] Zhao F, Harnisch F, Schroerder U, Scholz F, Bogdanoff P, Herrmann I. Challenges and constraints of using oxygen cathodes in microbial fuel cells. Environ Sci Technol 2006;40(17):5193–9.
[105] Gohil JM, Karamanev DG. Novel approach for the preparation of ionic liquid/ imidazoledicarboxylic acid modified poly(vinyl alcohol) polyelectrolyte membranes. J Membr Sci 2016;513:33–9.
[106] Leong JX, Daud WRW, Ghasemi M, Ahmad A, Ismail M, Ben Liew K. Composite membrane containing graphene oxide in sulfonated polyether ether ketone in microbial fuel cell applications. Int J Hydrogen Energy 2015;40 (35):11604–14.
[107] Lee Y-Y, Kim TG, Cho K. Effects of proton exchange membrane on the performance and microbial community composition of air-cathode microbial fuel cells. J Biotechnol 2015;10(211):130–7.
[108] Hernandez-Flores G, Poggi-Varaldo HM, Solorza-Feria O, Romero-Castanon T, Rios-Leal E, Galindez-Mayer J, et al. Batch operation of a microbial fuel cell equipped with alternative proton exchange membrane. Int J Hydrogen Energy 2015;40(48):17323–31.
[109] Hernandez-Fernandez FJ, Perez de los Rios A, Mateo-Ramirez F, Godinez C, Lozano-Blanco LJ, Moreno JI, et al. New application of supported ionic liquids membranes as proton exchange membranes in microbial fuel cell for waste water treatment. Chem Eng J 2015;279:115–9.
[110] Torres CI, Marcus AK, Rittmann BE. Proton transport inside the biofilm limits electrical current generation by anode-respiring bacteria. Biotechnol Bioeng 2008;100(5):872–81.
[111] Kim BH, Chang IS, Gadd GM. Challenges in microbial fuel cell development and operation. Appl Microbiol Biotechnol 2007;76(3):485–94.
[112] Ye Y, Zhu X, Logan BE. Effect of buffer charge on performance of air-cathodes used in microbial fuel cells. Electrochim Acta 2016;194:441–7.
[113] Le Bonté S, Pons M-N, Potier O, Rocklin P. Relation between conductivity and ion content in urban wastewater. J Water Sci 2008;21(4):429–38.
[114] Cao X, Huang X, Liang P, Xiao K, Zhou Y, Zhang X, et al. A new method for water desalination using microbial desalination cells. Environ Sci Technol 2009;43(18):7148–52.
[115] Kim Y, Logan BE. Series assembly of microbial desalination cells containing stacked electrodialysis cells for partial or complete seawater desalination. Environ Sci Technol 2011;45(13):5840–5.
[116] Shehab NA, Amy GL, Logan BE, Saikaly PE. Enhanced water desalination efficiency in an air-cathode stacked microbial electrodeionization cell (SMEDIC). J Membr Sci 2014;1(469):364–70.
[117] Nam J-Y, Jwa E, Kim D, Park S-C, Jeong N. Selective removal of multivalent ions from seawater by bioelectrochemical system. Desalination 2015;2 (359):37–40.
[118] Cusick RD, Kim Y, Logan BE. Energy capture from thermolytic solutions in microbial reverse-electrodialysis cells. Science 2012;335(6075): 1474–7.
[119] Liu J, Geise GM, Luo X, Hou H, Zhang F, Feng Y, et al. Patterned ion exchange membranes for improved power production in microbial reverse-electrodialysis cells. J Power Sources 2014;20(271):437–43.
[120] Clauwaert P, Rabaey K, Aelterman P, De Schamphelaire L, Ham TH, Boeckx P, et al. Biological denitrification in microbial fuel cells. Environ Sci Technol 2007;41(9):3354–60.
[121] Virdis B, Rabaey K, Yuan Z, Keller J. Microbial fuel cells for simultaneous carbon and nitrogen removal. Water Res 2008;42(12):3013–24.
[122] Kuntke P, Smiech KM, Bruning H, Zeeman G, Saakes M, Sleutels THJA, et al. Ammonium recovery and energy production from urine by a microbial fuel cell. Water Res 2012;46(8):2627–36.
[123] Kelly PT, He Z. Nutrients removal and recovery in bioelectrochemical systems: a review. Bioresour Technol 2014;153:351–60.
[124] Modin O, Fukushi K, Rabaey K, Rozendal RA, Yamamoto K. Redistribution of wastewater alkalinity with a microbial fuel cell to support nitrification of reject water. Water Res 2011;45(8):2691–9.
[125] Krieg T, Sydow A, Schroeder U, Schrader J, Holtmann D. Reactor concepts for bioelectrochemical syntheses and energy conversion. Trends Biotechnol 2014;32(12):645–55.
[126] Fan Y, Hu H, Liu H. Enhanced Coulombic efficiency and power density of air-cathode microbial fuel cells with an improved cell configuration. J Power Sources 2007;171(2):348–54.
[127] Fan Y, Han S-K, Liu H. Improved performance of CEA microbial fuel cells with increased reactor size. Energy Environ Sci 2012;5(8):8273–80.
[128] Abourached C, Lesnik KL, Liu H. Enhanced power generation and energy conversion of sewage sludge by CEA-microbial fuel cells. Bioresour Technol 2014;166:229–34.
[129] Greenlee LF, Lawler DF, Freeman BD, Marrot B, Moulin P. Reverse osmosis desalination: water sources, technology, and today's challenges. Water Res 2009;43(9):2317–48.
[130] Remigy J-C, Desclaux S. Filtration membranaire (OI, NF, UF) - Présentation des membranes et modules. Tech Ing 2007:W4090.
[131] Xu TW. Ion exchange membranes: state of their development and perspective. J Membr Sci 2005;263(1–2):1–29.
[132] Harnisch F, Schroder U, Scholz F. The suitability of monopolar and bipolar ion exchange membranes as separators for biological fuel cells. Environ Sci Technol 2008;42(5):1740–6.
[133] Kim JR, Cheng S, Oh S-E, Logan BE. Power generation using different cation, anion, and ultrafiltration membranes in microbial fuel cells. Environ Sci Technol 2007;41(3):1004–9.
[134] Chae KJ, Choi M, Ajayi FF, Park W, Chang IS, Kim IS. Mass transport through a proton exchange membrane (Nafion) in microbial fuel cells. Energy Fuels 2008;22(1):169–76.
[135] Khilari S, Pandit S, Ghangrekar MM, Pradhan D, Das D. Graphene oxide-impregnated PVA-STA composite polymer electrolyte membrane separator for power generation in a single-chambered microbial fuel cell. Ind Eng Chem Res 2013;52(33):11597–606.
[136] Venkatesan PN, Dharmalingam S. Effect of cation transport of SPEEK - rutile TiO_2 electrolyte on microbial fuel cell performance. J Membr Sci 2015;15 (492):518–27.
[137] Tao H-C, Sun X-N, Xiong Y. A novel hybrid anion exchange membrane for high performance microbial fuel cells. RSC Adv 2015;5(6):4659–63.
[138] Kondaveeti S, Lee J, Kakarla R, Kim HS, Min B. Low-cost separators for enhanced power production and field application of microbial fuel cells (MFCs). Electrochim Acta 2014;20(132):434–40.
[139] Moon JM, Kondaveeti S, Min B. Evaluation of low-cost separators for increased power generation in single chamber microbial fuel cells with membrane electrode assembly. Fuel Cells 2015;15(1):230–8.
[140] Sivasankaran A, Sangeetha D. Influence of sulfonated SiO_2 in sulfonated polyether ether ketone nanocomposite membrane in microbial fuel cell. Fuel 2015;1(159):689–96.
[141] Mahendiravarman E, Sangeetha D. Increased microbial fuel cell performance using quaternized poly ether ether ketone anionic membrane electrolyte for electricity generation. Int J Hydrogen Energy 2013;38(5):2471–9.
[142] Elangovan M, Dharmalingam S. Preparation and performance evaluation of poly (ether-imide) based anion exchange polymer membrane electrolyte for microbial fuel cell. Int J Hydrogen Energy 2016. http://dx.doi.org/10.1016/j.ijhydene.2016.03.185 [Internet].
[143] Ji E, Moon H, Piao J, Ha PT, An J, Kim D, et al. Interface resistances of anion exchange membranes in microbial fuel cells with low ionic strength. Biosens Bioelectron 2011;26(7):3266–71.
[144] Strathmann H, Grabowski A, Eigenberger G. Ion-exchange membranes in the chemical process industry. Ind Eng Chem Res 2013;52(31):10364–79.
[145] Malki M, De lacey AL, Rodrfguez N, Amils R, Fernandez VM. Preferential use of an anode as an electron acceptor by an acidophilic bacterium in the presence of oxygen. Appl Environ Microbiol 2008;74(14):4472–6.
[146] Sulonen MLK, Kokko ME, Lakaniemi A-M, Puhakka JA. Electricity generation from tetrathionate in microbial fuel cells by acidophiles. J Hazard Mater 2015;2(284):182–9.
[147] Rahimnejad M, Bakeri G, Ghasemi M, Zirepour A. A review on the role of proton exchange membrane on the performance of microbial fuel cell. Polym Adv Technol 2014;25(12):1426–32.
[148] Han L, Galier S, Roux-de Balmann H. Ion hydration number and electro-osmosis during electrodialysis of mixed salt solution. Desalination 2015;1 (373):38–46.
[149] Gajda I, Greenman J, Melhuish C, Santoro C, Li B, Cristiani P, et al. Electro-osmotic-based catholyte production by Microbial Fuel Cells for carbon capture. Water Res 2015;86:108–15.
[150] Mauritz KA, Moore RB. State of understanding of Nafion. Chem Rev 2004;104 (10):4535–85.
[151] Rahimnejad M, Jafary T, Haghparast F, Najafpour GD, Ghoreyshi AA. Nafion as a nanoproton conductor in microbial fuel cells. Turk J Eng Environ Sci 2010;34:289–92.
[152] Ghasemi M, Halakoo E, Sedighi M, Alam J, Sadeqzadeh M. Performance comparison of three common proton exchange membranes for sustainable bioenergy production in microbial fuel cell. In: Selige G, Yusof NM, editors. 12th Global conference on sustainable manufacturing - emerging potentials; 2015. p. 162–6.
[153] Pant D, Van Bogaert G, De Smet M, Diels L, Vanbroekhoven K. Use of novel permeable membrane and air cathodes in acetate microbial fuel cells. Electrochim Acta 2010;55(26):7710–6.
[154] Hernandez-Flores G, Poggi-Varaldo HM, Solorza-Feria O, Ponce-Noyola MT, Romero-Castanon T, Rinderknecht-Seijas N, et al. Characteristics of a single chamber microbial fuel cell equipped with a low cost membrane. Int J Hydrogen Energy 2015;40(48):17380–7.

[155] Xu J, Sheng G-P, Luo H-W, Li W-W, Wang L-F, Yu H-Q. Fouling of proton exchange membrane (PEM) deteriorates the performance of microbial fuel cell. Water Res 2012;46(6):1817–24.
[156] Ghasemi M, Daud WRW, Ismail M, Rahimnejad M, Ismail AF, Leong JX, et al. Effect of pre-treatment and biofouling of proton exchange membrane on microbial fuel cell performance. Int J Hydrogen Energy 2013;38(13):5480–4.
[157] Choi M-J, Chae K-J, Ajayi FF, Kim K-Y, Yu H-W, Kim C, et al. Effects of biofouling on ion transport through cation exchange membranes and microbial fuel cell performance. Bioresour Technol 2011;102(1):298–303.
[158] Mokhtarian N, Ghasemi M, Daud WRW, Ismail M, Najafpour G, Alam J. Improvement of microbial fuel cell performance by using nafion polyaniline composite membranes as a separator. J Fuel Cell Sci Technol 2013;10 (4):41008.
[159] Kamaraj S-K, Molla Romano S, Compan Moreno V, Poggi-Varaldo HM, Solorza-Feria O. Use of novel reinforced cation exchange membranes for microbial fuel cells. Electrochim Acta 2015;10(176):555–66.
[160] Ghasemi M, Daud WRW, Ismail AF, Jafari Y, Ismail M, Mayahi A, et al. Simultaneous wastewater treatment and electricity generation by microbial fuel cell: performance comparison and cost investigation of using Nafion 117 and SPEEK as separators. Desalination 2013;16(325):1–6.
[161] Chae K-J, Kim K-Y, Choi M-J, Yang E, Kim IS, Ren X, et al. Sulfonated polyether ether ketone (SPEEK)-based composite proton exchange membrane reinforced with nanofibers for microbial electrolysis cells. Chem Eng J 2014;15(254):393–8.
[162] Ghasemi M, Shahgaldi S, Ismail M, Yaakob Z, Daud WRW. New generation of carbon nanocomposite proton exchange membranes in microbial fuel cell systems. Chem Eng J 2012;1(184):82–9.
[163] Sivasankaran A, Sangeetha D, Ahn Y-H. Nanocomposite membranes based on sulfonated polystyrene ethylene butylene polystyrene (SSEBS) and sulfonated SiO_2 for microbial fuel cell application. Chem Eng J 2016;1 (289):442–51.
[164] Elangovan M, Dharmalingam S. A facile modification of a polysulphone based anti biofouling anion exchange membrane for microbial fuel cell application. RSC Adv 2016;6(25):20571–81.
[165] Pandit S, Sengupta A, Kale S, Das D. Performance of electron acceptors in catholyte of a two-chambered microbial fuel cell using anion exchange membrane. Bioresour Technol 2011;102(3):2736–44.
[166] Pandit S, Ghosh S, Ghangrekar MM, Das D. Performance of an anion exchange membrane in association with cathodic parameters in a dual chamber microbial fuel cell. Int J Hydrogen Energy 2012;37(11):9383–92.
[167] Piao J, An J, Ha PT, Kim T, Jang JK, Moon H, et al. Power density enhancement of anion-exchange membrane-installed microbial fuel cell under bicarbonate-buffered cathode condition. J Microbiol Biotechnol 2013;23 (1):36–9.
[168] Zuo Y, Cheng S, Logan BE. Ion exchange membrane cathodes for scalable microbial fuel cells. Environ Sci Technol 2008;42(18):6967–72.
[169] Mo Y, Liang P, Huang X, Wang H, Cao X. Enhancing the stability of power generation of single-chamber microbial fuel cells using an anion exchange membrane. J Chem Technol Biotechnol 2009;84(12):1767–72.
[170] Zhang X, Cheng S, Huang X, Logan BE. Improved performance of single-chamber microbial fuel cells through control of membrane deformation. Biosens Bioelectron 2010;25(7):1825–8.
[171] Ter Heijne A, Hamelers HVM, De Wilde V, Rozendal RA, Buisman CJN. A bipolar membrane combined with ferric iron reduction as an efficient cathode system in microbial fuel cells. Environ Sci Technol 2006;40 (17):5200–5.
[172] Ter Heijne A, Hamelers HVM, Buisman CJN. Microbial fuel cell operation with continuous biological ferrous iron oxidation of the catholyte. Environ Sci Technol 2007;41(11):4130–4.
[173] Chen M, Zhang F, Zhang Y, Zeng RJ. Alkali production from bipolar membrane electrodialysis powered by microbial fuel cell and application for biogas upgrading. Appl Energy 2013;103:428–34.
[174] Fradler KR, Michie F, Dinsdale RM, Guwy AJ, Premier GC. Augmenting microbial fuel cell power by coupling with supported liquid membrane permeation for zinc recovery. Water Res 2014;15(55):115–25.
[175] Kim E-S, Liu Y, El-Din MG. The effects of pretreatment on nanofiltration and reverse osmosis membrane filtration for desalination of oil sands process-affected water. Sep Purif Technol 2011;81(3):418–28.
[176] Tang F, Hu H-Y, Sun L-J, Wu Q-Y, Jiang Y-M, Guan Y-T, et al. Fouling of reverse osmosis membrane for municipal wastewater reclamation: autopsy results from a full-scale plant. Desalination 2014;15(349):73–9.
[177] Jia Z, Wang B, Song S, Fan Y. Blue energy: current technologies for sustainable power generation from water salinity gradient. Renew Sustain Energy Rev 2014;31:91–100.
[178] Naghiloo A, Abbaspour M, Mohammadi-Ivatloo B, Bakhtari K. Modeling and design of a 25 MW osmotic power plant (PRO) on Bahmanshir River of Iran. Renew Energy 2015;78:51–9.
[179] Xu P, Bellona C, Drewes JE. Fouling of nanofiltration and reverse osmosis membranes during municipal wastewater reclamation: membrane autopsy results from pilot-scale investigations. J Membr Sci 2010;353(1–2):111–21.
[180] Fathima NN, Aravindhan R, Lawrence D, Yugandhar U, Moorthy TSR, Nair BU. SPEEK polymeric membranes for fuel cell application and their characterization: a review. J Sci Ind Res 2007;66(3):209–19.
[181] Qin M, Ping Q, Lu Y, Abu-Reesh IM, He Z. Understanding electricity generation in osmotic microbial fuel cells through integrated experimental investigation and mathematical modeling. Bioresour Technol 2015;195:194–201.
[182] Werner CM, Logan BE, Saikaly PE, Amy GL. Wastewater treatment, energy recovery and desalination using a forward osmosis membrane in an air-cathode microbial osmotic fuel cell. J Membr Sci 2013;1(428):116–22.
[183] Yang E, Chae K-J, Alayande AB, Kim K-Y, Kim IS. Concurrent performance improvement and biofouling mitigation in osmotic microbial fuel cells using a silver nanoparticle-polydopamine coated forward osmosis membrane. J Membr Sci 2016. http://dx.doi.org/10.1016/j.memsci.2016.04.028 [Internet].
[184] Hoek EMV, Elimelech M. Cake-enhanced concentration polarization: a new fouling mechanism for salt-rejecting membranes. Environ Sci Technol 2003;37(24):5581–8.
[185] Tran T, Bolto B, Gray S, Hoang M, Ostarcevic E. An autopsy study of a fouled reverse osmosis membrane element used in a brackish water treatment plant. Water Res 2007;41(17):3915–23.
[186] Ge Z, Ping Q, Xiao L, He Z. Reducing effluent discharge and recovering bioenergy in an osmotic microbial fuel cell treating domestic wastewater. Desalination 2013;1(312):52–9.
[187] Ghadge AN, Ghangrekar MM. Development of low cost ceramic separator using mineral cation exchanger to enhance performance of microbial fuel cells. Electrochim Acta 2015;1(166):320–8.
[188] Tang X, Guo K, Li H, Du Z, Tian J. Microfiltration membrane performance in two-chamber microbial fuel cells. Biochem Eng J 2010;52(2–3):194–8.
[189] Baker RW. Membrane technology and applications. 3rd ed.; 2012. p. 223.
[190] Baker RW. Membrane technology and applications. 3rd ed. Wiley; 2012. p. 255.
[191] Van der Bruggen B, Koninckx A, Vandecasteele C. Separation of monovalent and divalent ions from aqueous solution by electrodialysis and nanofiltration. Water Res 2004;38(5):1347–53.
[192] Darbi A, Viraraghavan T, Jin YC, Braul L, Corkal D. Sulfate removal from water. Water Qual Res J Can 2003;38(1):169–82.
[193] Paugam L, Taha S, Cabon J, Dorange G. Elimination of nitrate ions in drinking waters by nanofiltration. Desalination 2003;152(1–3):271–4.
[194] Garcia F, Ciceron D, Saboni A, Alexandrova S. Nitrate ions elimination from drinking water by nanofiltration: membrane choice. Sep Purif Technol 2006;52(1):196–200.
[195] Vrijenhoek EM, Waypa JJ. Arsenic removal from drinking water by a "loose" nanofiltration membrane. Desalination 2000;130(3):265–77.
[196] Choo KH, Kwon DJ, Lee KW, Choi SJ. Selective removal of cobalt species using nanofiltration membranes. Environ Sci Technol 2002;36(6):1330–6.
[197] Kim K-Y, Chae K-J, Choi M-J, Yang E-T, Hwang MH, Kim IS. High-quality effluent and electricity production from non-CEM based flow-through type microbial fuel cell. Chem Eng J 2013;15(218):19–23.
[198] Hou B, Sun J, Hu Y. Simultaneous Congo red decolorization and electricity generation in air-cathode single-chamber microbial fuel cell with different microfiltration, ultrafiltration and proton exchange membranes. Bioresour Technol 2011;102(6):4433–8.
[199] Kim K-Y, Yang E, Lee M-Y, Chae K-J, Kim C-M, Kim IS. Polydopamine coating effects on ultrafiltration membrane to enhance power density and mitigate biofouling of ultrafiltration microbial fuel cells (UF-MFCs). Water Res 2014;1 (54):62–8.
[200] Winfield J, Chambers LD, Rossiter J, Ieropoulos I. Comparing the short and long term stability of biodegradable, ceramic and cation exchange membranes in microbial fuel cells. Bioresour Technol 2013;148:480–6.
[201] Winfield J, Greenman J, Huson D, Ieropoulos I. Comparing terracotta and earthenware for multiple functionalities in microbial fuel cells. Bioprocess Biosyst Eng 2013;36(12):1913–21.
[202] Biffinger JC, Ray R, Little B, Ringeisen BR. Diversifying biological fuel cell designs by use of nanoporous filters. Environ Sci Technol 2007;41(4):1444–9.
[203] Sun J, Hu Y, Bi Z, Cao Y. Improved performance of air-cathode single-chamber microbial fuel cell for wastewater treatment using microfiltration membranes and multiple sludge inoculation. J Power Sources 2009;187 (2):471–9.
[204] Yousefi V, Mohebbi-Kalhori D, Samimi A, Salari M. Effect of separator electrode assembly (SEA) design and mode of operation on the performance of continuous tubular microbial fuel cells (MFCs). Int J Hydrogen Energy 2016;41(1):597–606.
[205] Zhang X, Cheng S, Huang X, Logan BE. The use of nylon and glass fiber filter separators with different pore sizes in air-cathode single-chamber microbial fuel cells. Energy Environ Sci 2010;3(5):659–64.
[206] Zhang X, Liang P, Shi J, Wei J, Huang X. Using a glass fiber separator in a single-chamber air-cathode microbial fuel cell shortens start-up time and improves anode performance at ambient and mesophilic temperatures. Bioresour Technol 2013;130:529–35.
[207] Winfield J, Ieropoulos I, Rossiter J, Greenman J, Patton D. Biodegradation and proton exchange using natural rubber in microbial fuel cells. Biodegradation 2013;24(6):733–9.
[208] Winfield J, Chambers LD, Rossiter J, Stinchcombe A, Walter XA, Greenman J, et al. Fade to green: a biodegradable stack of microbial fuel cells. Chemsuschem 2015;8(16):2705–12.